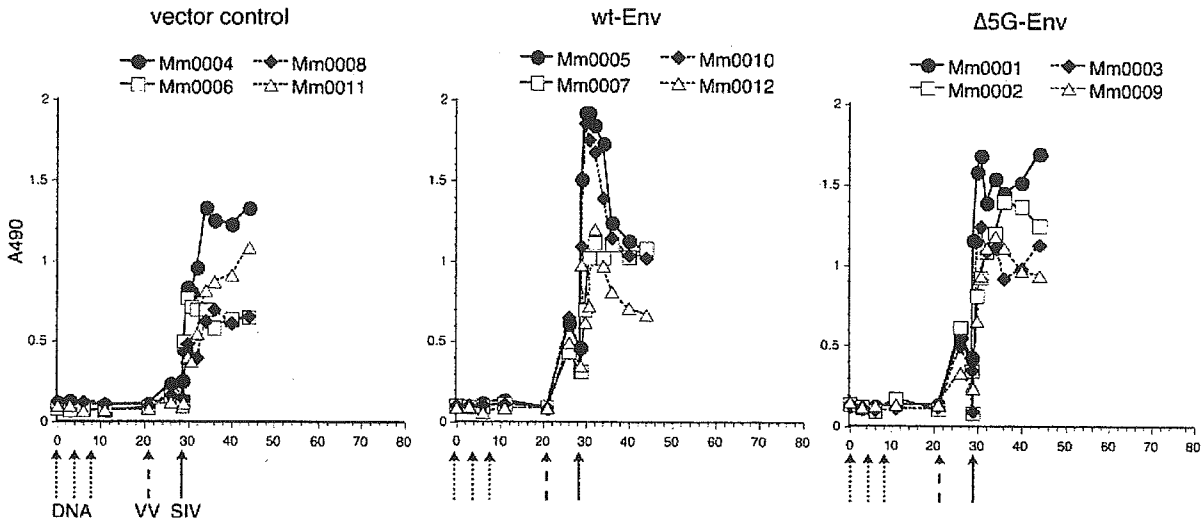

FIG. 4. Humoral immune response during immunization and after challenge infection. The OD_{492} was used as a relative measurement of anti-SIV ELISA antibody titer.

vaccinees were markedly reduced (Fig. 5B). Peak viral loads at 2 weeks p.i. (mean, 1×10^6 copies/ml; range, 0.8×10^6 to 1.2×10^6 copies/ml) were 1-log lower than those in the vector controls. Furthermore, viral loads decreased to as low as 1,000 copies/ml by 8 to 20 weeks p.i., remaining low until autopsy at 45 weeks p.i.

Unexpectedly, viral loads in the Δ5G Env vaccine group resembled those in vector controls (Fig. 5C). Peak viral loads (mean, 2.4×10^6 copies/ml; range, 0.9×10^6 to 4.2×10^6 copies/ml) were slightly lower than those in vector controls. Set points and viral loads in the chronic phase were similar to those of vector controls.

In summary, as shown by the mean viral loads in primary and chronic infection (Fig. 5D) and statistical analysis (Fig. 5E), the effects of vaccination differed between the wt-Env vaccine and Δ5G Env vaccine. In the effect on primary infection (up to 6 weeks p.i.), wt-Env vaccination decreased viral loads more extensively and significantly than Δ5G Env vaccination (P = 0.029 versus P = 0.057); however, in chronic infection (viral loads after 8 weeks p.i.), significant reductions in viral loads compared with those in vector controls were seen only in the wt-Env vaccine group and not the Δ5G Env vaccine group (Fig. 5E). Collectively, wt-Env vaccination induced significantly effective immunity to control SIVmac239 infection, whereas Δ5G Env vaccination induced a marginal effect seen only in primary and not in chronic infection.

TABLE 1. Neutralizing-antibody titers in the vaccinated macaques at 26 weeks p.p.

Vaccine	Animal	Neutralizing-antibody titer[a]			Mean[b]
		SIVmac239	Δ5G	239/envMERT	
wt-Env	Mm0005	<20	<20	800	400
	Mm0007	<20	<20	400	
	Mm0010	<20	<20	400	
	Mm0012	<20	<20	200	
Δ5G-Env	Mm0001	<20	<20	100	50
	Mm0002	<20	<20	20	
	Mm0003	<20	<20	100	
	Mm0009	<20	<20	50	

[a] Reciprocal of the dilution of plasma giving 50% inhibition of SIV replication.
[b] The difference in NAb levels between the two vaccine groups was significant (P = 0.0029).

$CD4^+$ T-cell subsets in PBMCs. CD4 cell depletion is a primary manifestation indicating immune disorder in HIV/SIV infection. As CD4 depletion results from HIV/SIV infection in lymphatic tissue, it correlates with the extent of viral replication. Accordingly, viral loads were correlated mostly with CD4 depletion (Fig. 5 and 6A). Despite fluctuations due to immunizations and the challenge infection, the percentage of $CD4^+$ T cells in wt-Env-immunized animals in the chronic phase recovered to the levels at the initiation of the experiment. By contrast, in vector controls and Δ5G Env vaccinees, the percentage of $CD4^+$ T cells decreased in the chronic phase. Among them, an extensive decrease in $CD4^+$ T cells occurred in animals with high viral loads in the chronic phase (Mm0001, Mm0008, and Mm0009) (Fig. 5 and 6A). However, in the other animals, the levels of $CD4^+$ T cells remained as before the challenge (Mm0003, Mm0011).

A subset of $CD4^+$ CD29 high cells, approximately corresponding to memory $CD4^+$ T cells, is useful for diagnosing a deterioration in the immune function in animals with AIDS (26, 38, 48). Although this parameter usually correlates with the percentage of $CD4^+$ T cells, remarkable differences were noted between two Env vaccine groups after the challenge infection. First, all animals in the wt-Env vaccine group showed an increased percentage of this subset in the chronic phase (Fig. 6B). Second, three of the Δ5G Env vaccinees had a marked decrease after the challenge infection (Mm0001, Mm0002 and Mm0009), whereas the remaining animal (Mm0003) showed an increased percentage of this subset. In

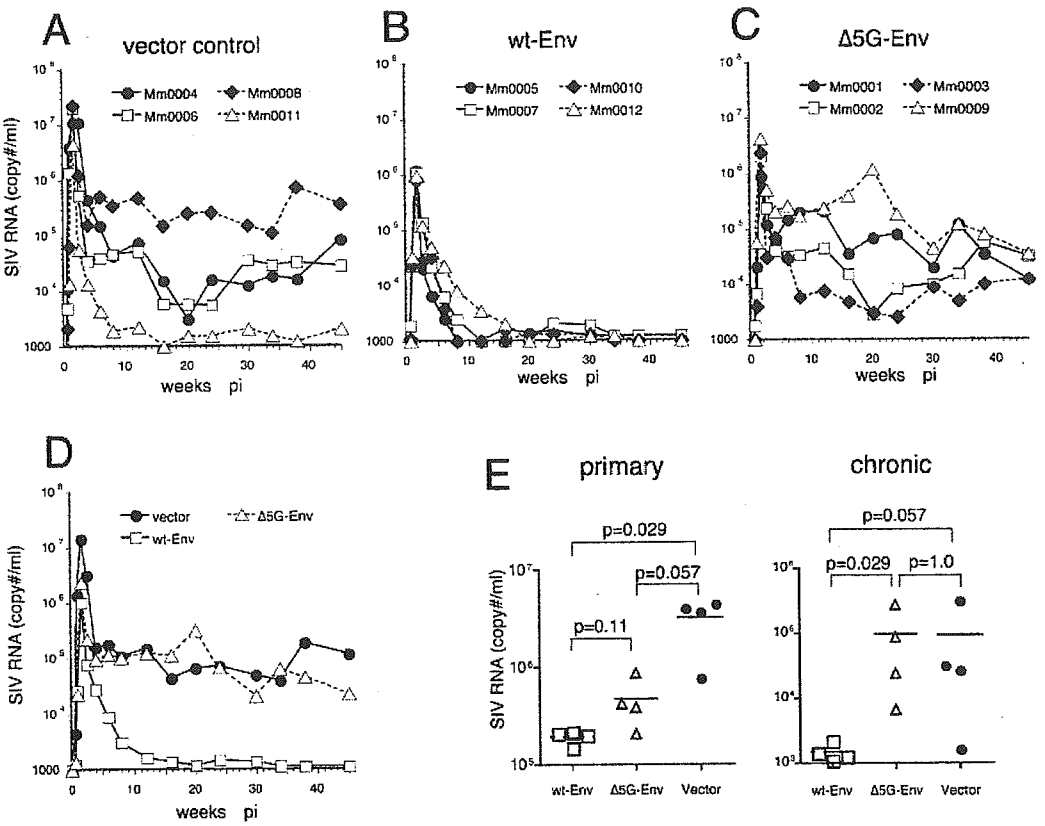

FIG. 5. Plasma viral loads after SIVmac239 challenge infection. Plasma viral load was measured by real-time PCR with a detection limit of 1,000 copies/ml. A: wt-Env vaccine group; B: Δ5G Env vaccine group; C: vector controls; D: comparison of viral loads among three groups; E: comparison of viral loads during the primary infection (5 days to 6 weeks p.i.) and chronic infection (8 weeks to 45 weeks p.i.) among three groups. Viral load was determined by averaging over a period of time.

vector controls, this subset remained in the range before the challenge infection in all animals but one (Fig. 6B).

Env-specific-T-cell immunity after the challenge infection. The magnitude of Env-specific T cells after the challenge infection is assumed to be influenced not only by vaccination but also by viral replication. Namely, SU-specific T cells at 4 days p.i. and those at 12 days p.i. were likely influenced by the former and the latter respectively. The magnitudes of SU-specific $CD4^+$ T cells and $CD8^+$ T cells at 4 days p.i. were comparable to those before challenge at 26 weeks p.p. (Fig. 3A and B); therefore, twofold-more SU-specific $CD8^+$ T cells and $CD4^+$ T cells were present in wt-Env vaccinees than in Δ5G Env vaccinees up to 4 days p.i. (Fig. 3C). However, this difference in the magnitudes of SU-specific $CD8^+$ T and $CD4^+$ T cells was not sustained at 7 and 12 days p.i. (Fig. 3C). Present with robust viral replication in primary infection, SU-specific $CD4^+$ T cells immediately decreased to an undetectable level at 12 days p.i. In contrast, SU-specific $CD8^+$ T cells increased (Fig. 3A and B). Subsequently, SU-specific $CD8^+$ T cells gradually decreased to very low or undetectable levels by 34 weeks p.i. (Fig. 3A). Thus, vaccine-induced SU-specific $CD8^+$ T and $CD4^+$ T cells were sustained only for a short period of time after challenge infection in both Env vaccine groups.

SIV-specific T-cell immunity after challenge infection. Despite an Env vaccination, robust SIV infection occurred shortly after the challenge infection (Fig. 5B and C). Consequently, SIV-specific $CD8^+$ T cells and $CD4^+$ T cells were elicited not only in vector controls but also in Env vaccine groups (Fig. 7A and B). To examine the effect of these SIV-specific T cells on the control of SIV infection, all animals were divided into SIV infection-controlled (controlled) and SIV infection-uncontrolled (uncontrolled) animals. Viral loads in chronic infection and the percentage of $CD4^+$ cells in PBMCs were used to classify the animals as controlled or uncontrolled (Fig. 6A). All animals in the wt-Env vaccine group, Mm00011 in vector controls, and Mm0003 in the Δ5G Env vaccine group were grouped as control animals. The remaining animals, Mm0004, Mm0006, and Mm0008 in vector controls and Mm0001, Mm0002, and Mm0009 in the Δ5G Env vaccine group were grouped as uncontrolled animals. Notably, SIV-specific $CD4^+$ T cells as well as the percentage of $CD4^+$ CD29H cells remained high in the chronic phase in controlled animals (Fig. 7B and 6B, respectively).

Although overall SIV-specific $CD8^+$ T cells were high in Env-vaccinated controlled animals, such correlation was not seen in vector controls grouped as uncontrolled animals (Fig. 7A). Therefore, to examine the relevance of virus-specific T cells to the control of SIV infection, the magnitudes of every viral-protein-specific T cell in controlled and uncontrolled animals were compared. As shown in Fig. 7C, Gag-specific $CD8^+$ T cells and $CD4^+$ T cells, and Tat/Rev-specific $CD4^+$ T cells

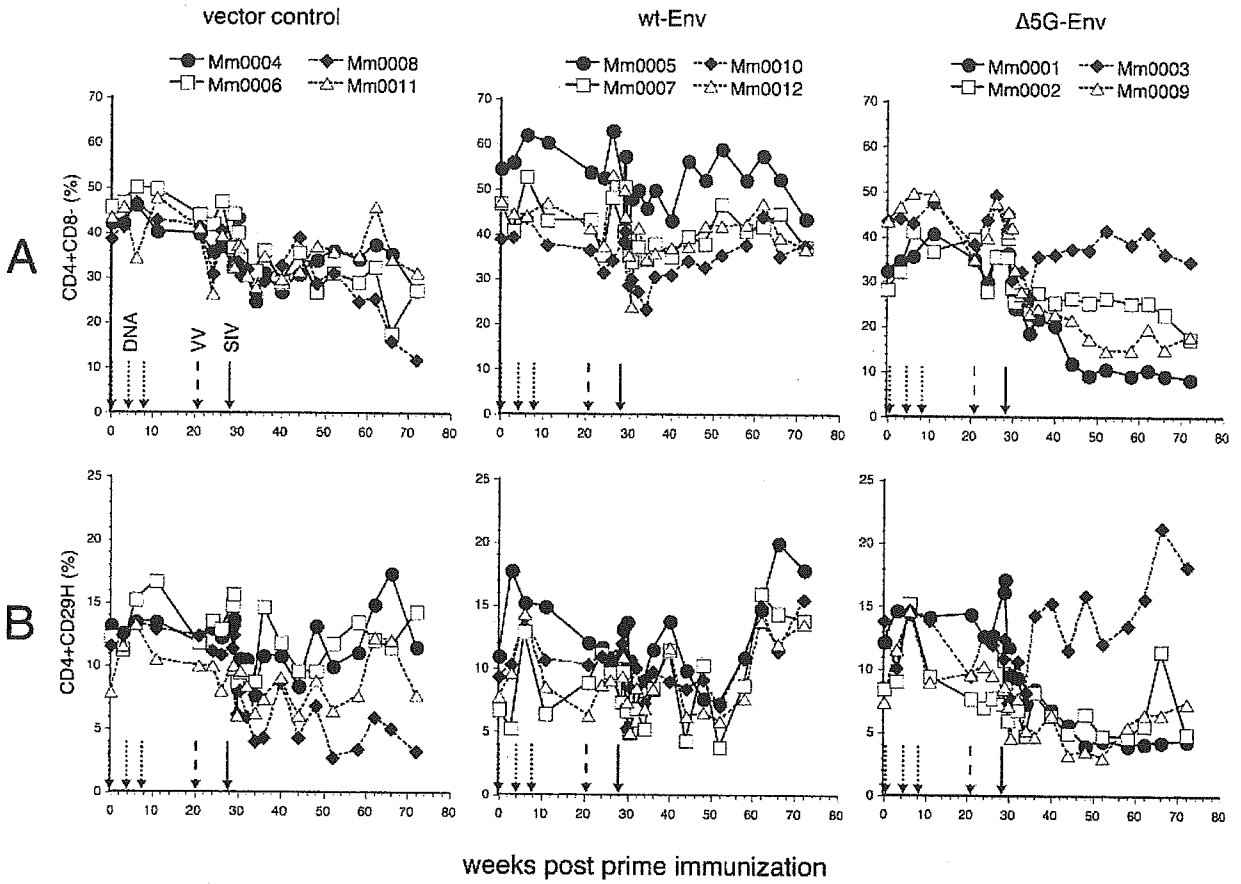

FIG. 6. $CD4^+$ T cells in PBMCs from rhesus macaques during immunization and after the challenge infection. A: Percentage of $CD4^+$ T cells in PBMCs; B: percentage of $CD4^+$ CD29high T cells in PBMCs.

were induced, with statistical significance ($P < 0.05$), in the control animals.

DISCUSSION

The heavily glycosylated structure of Env has been considered a main cause of chronically persistent viral replication and the pathogenicity of HIV/SIV, primarily because it potentially interferes with the development of the host immune response associated with protective immune functions, such as NAb and CTL (10, 36, 44). This characteristic constitutes the primary reason for the difficulty of developing effective vaccines. We therefore examined the efficacy of a deglycosylated-Env vaccine and compared it with the wt-Env vaccine. This study showed that quintuple deglycosylation neither improved the immunogenicity of the wt-Env vaccine nor elicited NAb against SIVmac239. This was in contrast to what occurred with Δ5G infection in rhesus macaques, because the host response elicited by Δ5G infection not only contained Δ5G infection but also protected the animals from SIVmac239 challenge infection (36). This study therefore suggested that an almost sterilizing immunity against SIVmac239 induced in Δ5G-infected animals could not be explained by the immunogenicity of Δ5G Env; instead, it is likely associated with the property of Δ5G as an attenuated virus. In fact, Δ5G was more neutralization-sensitive than SIVmac239 (36). Alternatively, the immunogenic property of Env in Δ5G could not successfully be duplicated by immunization with a Δ5G Env DNA prime-vaccinia virus boost regimen. Therefore, another immunization regimen might be able to elicit the protective immune response induced by Δ5G infection.

The Env vaccine is superior to other vaccines containing other viral proteins with respect to the induction of NAb; however, both the Δ5G Env vaccine and the wt-Env vaccine could not induce detectable NAb against either SIVmac239 or Δ5G. Instead, the wt-Env vaccine induced higher NAb against macrophage-tropic SIV than the Δ5G Env vaccine. Notably, this parameter most significantly correlated with the efficacies of the two Env vaccines. As Ab neutralized the macrophage-tropic variant 239/envMERT, which has only four separate amino acid substitutions distributed in *env* of SVmac239 (34), it might recognize unknown epitopes conserved between SIVmac239 and 239/envMERT. On the other hand, Δ5G Env may not sufficiently present this epitope due to mutations. Regarding the role of nonneutralizing Ab for the control of SIVmac239 infection, it is assumed that, as the neutralization assay did not necessarily reflect in vivo conditions, such nonneutralizing Ab with potential virus-binding ability may interfere with SIVmac239 infection in animals. Alternatively, Ab

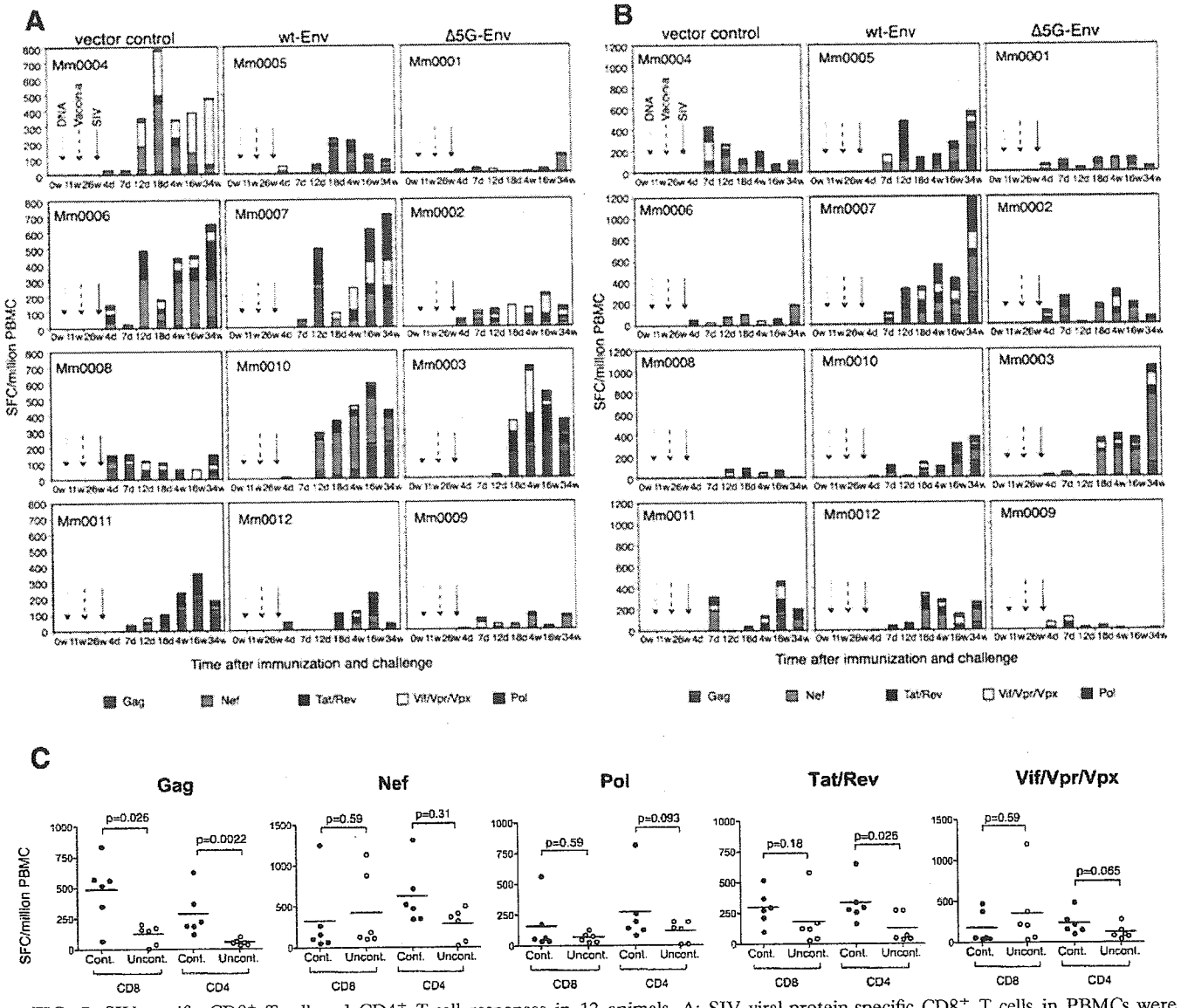

FIG. 7. SIV-specific $CD8^+$ T-cell and $CD4^+$ T-cell responses in 12 animals. A: SIV viral-protein-specific $CD8^+$ T cells in PBMCs were measured by ELISPOT assay for IFN-γ in three groups: vector controls, wt-Env vaccine group, and Δ5G Env vaccines. B: SIV viral-protein-specific $CD4^+$ T cells in PBMCs were measured by ELISPOT assay for IFN-γ in three groups. ELISPOT results of individual SIV proteins are colored as follows: Gag (red), Nef (green), Tat/Rev (blue), Vif/Vpr/Vpx (yellow), and Pol (pink). C: Comparison of cumulated $CD8^+$ T cells or $CD4^+$ T cells specific to the viral proteins Gag, Pol, Nef, Tat/Rev, and Vif/Vpr/VpX between SIV infection-controlled and uncontrolled animals. w, weeks; d, days.

might play a role in other effector functions, such as antibody-dependent cell-mediated cytotoxicity to eliminate the infected cells. The antibody-mediated enhancement of viral antigen processing and cross presentation is also a mechanism potentially related to the control of SIV infection in vivo (49).

Reduced immunogenicity in the Δ5G Env vaccine was also noted in cellular immunity. The levels of stimulation of antigen-specific $CD8^+$ T cells and $CD4^+$ T cells are MHC I and MHC II dependent, respectively. As the macaques in this study have different MHC haplotypes (data not shown), the magnitude and breadth of SIV-specific T cells should vary among the animals. Nevertheless, the magnitude of SU-specific $CD8^+$ T cells and $CD4^+$ T cells in PBMCs was greater in the wt-Env vaccine group than in the Δ5G Env vaccine group. Although the expression of SU by expressing plasmids and that of Env by the vaccinia virus vector elicited by either the wt-Env vaccine or Δ5G Env vaccine were indistinguishable in cultured cells (Fig. 2), wt-Env might persist longer than Δ5G Env in vaccinated animals. T-cell epitopes in the wt-Env vaccine might therefore be more efficiently presented on MHC molecules in antigen-presenting cells than in the Δ5G Env vaccine. Differences in glycosylation levels might also affect some processes in antigen-presenting cells associated with the presentation of T-cell epitopes in Env.

Taking all results together, Env glycosylation might affect the presentation of B-cell epitopes and T-cell epitopes required for Ab-mediated and T-cell-mediated immunities related to the control of SIV infection.

As seen in viral loads and SU-specific T cell levels after challenge infection (Fig. 3 and 5), the effect of vaccination was limited. That seemed related to the development of escape mutants. Therefore, distinctive cellular immune responses after the challenge infection were also implicated in the control of SIVmac239 replication. The magnitude of virus-specific $CD8^+$ T cells did not always correlate with the suppression of viral replication as reported previously (1, 6), particularly in vector controls (Fig. 5 and 7A); however, selected epitope-specific CTL responses might be associated with infection control. Gag-specific CTLs are such candidates, because a high magnitude of Gag-specific $CD8^+$ T cells was significantly elicited in five control animals (Fig. 7C). The magnitude of Gag- or Tat/Rev-specific $CD4^+$ T cells was statistically correlated with infection control (Fig. 7C). This may simply indicate a lower depletion of virus-specific $CD4^+$ T cells in animals with lower viral loads as reported previously (11). Alternatively, these virus-specific $CD4^+$ T cells may play an important role in protective immunity (39). Taken together, these results implicated the dominant role of selected epitope-specific $CD4^+$ T cells and $CD8^+$ T cells for the control of SIVmac239 infection.

The challenge virus that should be used has been an important issue in AIDS vaccine studies (8, 10, 12). Many studies have reported impressive efficacy in a pathogenic-SHIV macaque model (3, 4, 45, 46); however, pathogenic SHIVs use CXCR4 as a coreceptor, whereas the majority of clinical isolates of HIV-1 use CCR5 (13, 27). Therefore, the challenge virus for an AIDS vaccine study should be an R5 virus, such as SIV (10). Consistent with this concern, a DNA prime–modified-vaccinia virus Ankara boost regimen, inducing broad SIV-specific T-cell responses, reduced the initial viral replication but did not prevent disease progression against SIVmac239 challenge (18). Thus, vaccine studies using pathogenic SHIV should be reevaluated by using an R5 virus (10).

Matano et al. reported that a DNA prime-Sendai virus boost regimen induced the CTL-based control of SIVmac239 in rhesus macaques (27). This study demonstrated that a DNA prime-vaccinia virus WR boost regimen expressing only Env controlled the chronic infection of SIVmac239 in rhesus macaques. The relatively lower viral loads in macaques from Myanmar or Laos than in those of Indian origin might contribute to the control of SIVmac239 infection. Nevertheless, it is important that these two studies demonstrated the efficacies of the two vaccine regimens against highly pathogenic SIVmac239. In earlier studies, other R5 SIVs were used as a challenge virus for an efficacy study of vaccine candidates. An Env-based vaccine in vaccinia virus vector priming and subunit protein boosting protected cynomologous macaques against homologous SIVmne clone E11S (42). In recombinant modified vaccinia virus, Ankara viruses expressing Gag-Pol and/or Env exhibited vaccine efficacy because of reduced viremia and the increased survival of rhesus macaques infected with uncloned SIVsmE660 (41). Accordingly, the efficacy of vaccine candidates might be influenced by the experimental conditions. Thus, well-defined animal models with detailed virological, immunological, and genetic information and suitable challenge viruses are required for the evaluation of vaccine candidates and the development of an AIDS vaccine.

This study demonstrated the importance of Env as a component of the AIDS vaccine, and Env-specific $CD8^+$ and $CD4^+$ T cells and nonneutralizing Env-specific Ab were suggested as protective immunity components. Quintuple deglycosylation in Env reduced vaccine efficacy and Env-specific immune responses. Env may therefore be comprised of appropriate antigenic properties to elicit humoral and cellular immune responses required for protective immunity against homologous or allele-specific target SIV/HIV. These properties could be modified by the alteration of glycosylation.

In conclusion, although Env is an important immunogen for the AIDS vaccine, Env properties, including glycosylation, should be carefully considered to design vaccines specific to the targeted viruses.

ACKNOWLEDGMENTS

We thank Kayoko Ueda for excellent technical assistance.

This work was supported by AIDS research grants from the Health Sciences Research Grants, from the Ministry of Health, Labor, and Welfare in Japan, and from the Ministry of Education, Culture, Sports, Science and Technology in Japan.

REFERENCES

1. **Addo, M. M., X. G. Yu, A. Rathod, D. Cohen, R. L. Eldridge, D. Strick, M. N. Johnston, C. Corcoran, A. G. Wurcel, C. A. Fitzpatrick, M. E. Feeney, W. R. Rodriguez, N. Basgoz, R. Draenert, D. R. Stone, C. Brander, P. J. Goulder, E. S. Rosenberg, M. Altfeld, and B. D. Walker.** 2003. Comprehensive epitope analysis of human immunodeficiency virus type 1 (HIV-1)-specific T-cell responses directed against the entire expressed HIV-1 genome demonstrate broadly directed responses, but no correlation to viral load. J. Virol. **77**:2081–2092.
2. **Allen, T. M., and D. I. Watkins.** 2001. New insights into evaluating effective T-cell responses to HIV. AIDS **15**(Suppl. 5):S117–S126.
3. **Amara, R. R., F. Villinger, J. D. Altman, S. L. Lydy, S. P. O'Neil, S. I. Staprans, D. C. Montefiori, Y. Xu, J. G. Herndon, L. S. Wyatt, M. A. Candido, N. L. Kozyr, P. L. Earl, J. M. Smith, H. L. Ma, B. D. Grimm, M. L. Hulsey, J. Miller, H. M. McClure, J. M. McNicholl, B. Moss, and H. L. Robinson.** 2001. Control of a mucosal challenge and prevention of AIDS by a multiprotein DNA/MVA vaccine. Science **292**:69–74.
4. **Barouch, D. H., S. Santra, J. E. Schmitz, M. J. Kuroda, T. M. Fu, W. Wagner, M. Bilska, A. Craiu, X. X. Zheng, G. R. Krivulka, K. Beaudry, M. A. Lifton, C. E. Nickerson, W. L. Trigona, K. Punt, D. C. Freed, L. Guan, S. Dubey, D. Casimiro, A. Simon, M. E. Davies, M. Chastain, T. B. Strom, R. S. Gelman, D. C. Montefiori, M. G. Lewis, E. A. Emini, J. W. Shiver, and N. L. Letvin.** 2000. Control of viremia and prevention of clinical AIDS in rhesus monkeys by cytokine-augmented DNA vaccination. Science **290**:486–492.
5. **Berger, E. A., P. M. Murphy, and J. M. Farber.** 1999. Chemokine receptors as HIV-1 coreceptors: roles in viral entry, tropism, and disease. Annu. Rev. Immunol. **17**:657–700.
6. **Betts, M. R., D. R. Ambrozak, D. C. Douek, S. Bonhoeffer, J. M. Brenchley, J. P. Casazza, R. A. Koup, and L. J. Picker.** 2001. Analysis of total human immunodeficiency virus (HIV)-specific CD4(+) and CD8(+) T-cell responses: relationship to viral load in untreated HIV infection. J. Virol. **75**:11983–11991.
7. **Burton, D. R.** 2002. Antibodies, viruses and vaccines. Nat. Rev. Immunol. **2**:706–713.
8. **Burton, D. R., R. C. Desrosiers, R. W. Doms, W. C. Koff, P. D. Kwong, J. P. Moore, G. J. Nabel, J. Sodroski, I. A. Wilson, and R. T. Wyatt.** 2004. HIV vaccine design and the neutralizing antibody problem. Nat. Immunol. **5**:233–236.
9. **Chapman, B. S., R. M. Thayer, K. A. Vincent, and N. L. Haigwood.** 1991. Effect of intron A from human cytomegalovirus (Towne) immediate-early gene on heterologous expression in mammalian cells. Nucleic Acids Res. **19**:3979–3986.
10. **Desrosiers, R. C.** 2004. Prospects for an AIDS vaccine. Nat. Med. **10**:221–223.
11. **Douek, D. C., J. M. Brenchley, M. R. Betts, D. R. Ambrozak, B. J. Hill, Y. Okamoto, J. P. Casazza, J. Kuruppu, K. Kunstman, S. Wolinsky, Z. Grossman, M. Dybul, A. Oxenius, D. A. Price, M. Connors, and R. A. Koup.** 2002. HIV preferentially infects HIV-specific CD4+ T cells. Nature **417**:95–98.
12. **Emini, E. A., and W. C. Koff.** 2004. AIDS/HIV. Developing an AIDS vaccine: need, uncertainty, hope. Science **304**:1913–1914.
13. **Feinberg, M. B., and J. P. Moore.** 2002. AIDS vaccine models: challenging challenge viruses. Nat Med. **8**:207–210.
14. **Gardner, M. B.** 2003. Simian AIDS: an historical perspective. J. Med. Primatol. **32**:180–186.
15. **Gotoh, H., T. Shioda, Y. Sakai, K. Mizumoto, and H. Shibuta.** 1989. Rescue

of Sendai virus from viral ribonucleoprotein-transfected cells by infection with recombinant vaccinia viruses carrying Sendai virus L and P/C genes. Virology **171**:434–443.
16. **Haigwood, N. L., and L. Stamatatos.** 2003. Role of neutralizing antibodies in HIV infection. AIDS **17**(Suppl. 4):S67–S71.
17. **Hirsch, V. M.** 2004. What can natural infection of African monkeys with simian immunodeficiency virus tell us about the pathogenesis of AIDS? AIDS Rev. **6**:40–53.
18. **Horton, H., T. U. Vogel, D. K. Carter, K. Vielhuber, D. H. Fuller, T. Shipley, J. T. Fuller, K. J. Kunstman, G. Sutter, D. C. Montefiori, V. Erfle, R. C. Desrosiers, N. Wilson, L. J. Picker, S. M. Wolinsky, C. Wang, D. B. Allison, and D. I. Watkins.** 2002. Immunization of rhesus macaques with a DNA prime/modified vaccinia virus Ankara boost regimen induces broad simian immunodeficiency virus (SIV)-specific T-cell responses and reduces initial viral replication but does not prevent disease progression following challenge with pathogenic SIVmac239. J. Virol. **76**:7187–7202.
19. **Johnson, R. P., R. L. Glickman, J. Q. Yang, A. Kaur, J. T. Dion, M. J. Mulligan, and R. C. Desrosiers.** 1997. Induction of vigorous cytotoxic T-lymphocyte responses by live attenuated simian immunodeficiency virus. J. Virol. **71**:7711–7718.
20. **Johnson, W. E., J. D. Lifson, S. M. Lang, R. P. Johnson, and R. C. Desrosiers.** 2003. Importance of B-cell responses for immunological control of variant strains of simian immunodeficiency virus. J. Virol. **77**:375–381.
21. **Johnson, W. E., H. Sanford, L. Schwall, D. R. Burton, P. W. Parren, J. E. Robinson, and R. C. Desrosiers.** 2003. Assorted mutations in the envelope gene of simian immunodeficiency virus lead to loss of neutralization resistance against antibodies representing a broad spectrum of specificities. J. Virol. **77**:9993–10003.
22. **Kano, M., T. Matano, A. Kato, H. Nakamura, A. Takeda, Y. Suzaki, Y. Ami, K. Terao, and Y. Nagai.** 2002. Primary replication of a recombinant Sendai virus vector in macaques. J. Gen. Virol. **83**:1377–1386.
23. **Kano, M., T. Matano, H. Nakamura, A. Takeda, A. Kato, K. Ariyoshi, K. Mori, T. Sata, and Y. Nagai.** 2000. Elicitation of protective immunity against simian immunodeficiency virus infection by a recombinant Sendai virus expressing the Gag protein. AIDS **14**:1281–1282.
24. **Letvin, N. L., J. E. Schmitz, H. L. Jordan, A. Seth, V. M. Hirsch, K. A. Reimann, and M. J. Kuroda.** 1999. Cytotoxic T lymphocytes specific for the simian immunodeficiency virus. Immunol. Rev. **170**:127–134.
25. **Lifson, J. D., M. A. Nowak, S. Goldstein, J. L. Rossio, A. Kinter, G. Vasquez, T. A. Wiltrout, C. Brown, D. Schneider, L. Wahl, A. L. Lloyd, J. Williams, W. R. Elkins, A. S. Fauci, and V. M. Hirsch.** 1997. The extent of early viral replication is a critical determinant of the natural history of simian immunodeficiency virus infection. J. Virol. **71**:9508–9514.
26. **Matano, T., M. Kano, T. Odawara, H. Nakamura, A. Takeda, K. Mori, T. Sato, and Y. Nagai.** 2000. Induction of protective immunity against pathogenic simian immunodeficiency virus by a foreign receptor-dependent replication of an engineered avirulent virus. Vaccine **18**:3310–3318.
27. **Matano, T., M. Kobayashi, H. Igarashi, A. Takeda, H. Nakamura, M. Kano, C. Sugimoto, K. Mori, A. Iida, T. Hirata, M. Hasegawa, T. Yuasa, M. Miyazawa, Y. Takahashi, M. Yasunami, A. Kimura, D. H. O'Connor, D. I. Watkins, and Y. Nagai.** 2004. Cytotoxic T lymphocyte-based control of simian immunodeficiency virus replication in a preclinical AIDS vaccine trial. J Exp. Med. **199**:1709–1718.
28. **McMichael, A. J., and S. L. Rowland-Jones.** 2001. Cellular immune responses to HIV. Nature **410**:980–987.
29. **Means, R. E., T. Greenough, and R. C. Desrosiers.** 1997. Neutralization sensitivity of cell culture-passaged simian immunodeficiency virus. J. Virol. **71**:7895–7902.
30. **Means, R. E., T. Matthews, J. A. Hoxie, M. H. Malim, T. Kodama, and R. C. Desrosiers.** 2001. Ability of the V3 loop of simian immunodeficiency virus to serve as a target for antibody-mediated neutralization: correlation of neutralization sensitivity, growth in macrophages, and decreased dependence on CD4. J. Virol. **75**:3903–3915.
31. **Mellors, J. W., L. A. Kingsley, C. R. Rinaldo, Jr., J. A. Todd, B. S. Hoo, R. P. Kokka, and P. Gupta.** 1995. Quantitation of HIV-1 RNA in plasma predicts outcome after seroconversion. Ann. Intern. Med. **122**:573–579.
32. **Moore, J. P., S. G. Kitchen, P. Pugach, and J. A. Zack.** 2004. The CCR5 and CXCR4 coreceptors—central to understanding the transmission and pathogenesis of human immunodeficiency virus type 1 infection. AIDS Res. Hum. Retrovir. **20**:111–126.
33. **Mori, K., D. J. Ringler, and R. C. Desrosiers.** 1993. Restricted replication of simian immunodeficiency virus strain 239 in macrophages is determined by Env but is not due to restricted entry. J. Virol. **67**:2807–2814.
34. **Mori, K., D. J. Ringler, T. Kodama, and R. C. Desrosiers.** 1992. Complex determinants of macrophage tropism in Env of simian immunodeficiency virus. J. Virol. **66**:2067–2075.
35. **Mori, K., M. Rosenzweig, and R. C. Desrosiers.** 2000. Mechanisms for adaptation of simian immunodeficiency virus to replication in alveolar macrophages. J. Virol. **74**:10852–10859.
36. **Mori, K., Y. Yasutomi, S. Ohgimoto, T. Nakasone, S. Takamura, T. Shioda, and Y. Nagai.** 2001. Quintuple deglycosylation mutant of simian immunodeficiency virus SIVmac239 in rhesus macaques: robust primary replication, tightly contained chronic infection, and elicitation of potent immunity against the parental wild-type strain. J. Virol. **75**:4023–4028.
37. **Mori, K., Y. Yasutomi, S. Sawada, F. Villinger, K. Sugama, B. Rosenwith, J. L. Heeney, K. Uberla, S. Yamazaki, A. A. Ansari, and H. Rubsamen-Waigmann.** 2000. Suppression of acute viremia by short-term postexposure prophylaxis of simian/human immunodeficiency virus SHIV-RT-infected monkeys with a novel reverse transcriptase inhibitor (GW420867) allows for development of potent antiviral immune responses resulting in efficient containment of infection. J. Virol. **74**:5747–5753.
38. **Munch, J., N. Adam, N. Finze, N. Stolte, C. Stahl-Hennig, D. Fuchs, P. Ten Haaft, J. L. Heeney, and F. Kirchhoff.** 2001. Simian immunodeficiency virus in which *nef* and U3 sequences do not overlap replicates efficiently in vitro and in vivo in rhesus macaques. J. Virol. **75**:8137–8146.
39. **Norris, P. J., and E. S. Rosenberg.** 2001. Cellular immune response to human immunodeficiency virus. AIDS **15**(Suppl. 2):S16–S21.
40. **Ohgimoto, S., T. Shioda, K. Mori, E. E. Nakayama, H. Hu, and Y. Nagai.** 1998. Location-specific, unequal contribution of the N glycans in simian immunodeficiency virus gp120 to viral infectivity and removal of multiple glycans without disturbing infectivity. J. Virol. **72**:8365–8370.
41. **Ourmanov, I., C. R. Brown, B. Moss, M. Carroll, L. Wyatt, L. Pletneva, S. Goldstein, D. Venzon, and V. M. Hirsch.** 2000. Comparative efficacy of recombinant modified vaccinia virus Ankara expressing simian immunodeficiency virus (SIV) Gag-Pol and/or Env in macaques challenged with pathogenic SIV. J. Virol. **74**:2740–2751.
42. **Polacino, P., V. Stallard, J. E. Klaniecki, D. C. Montefiori, A. J. Langlois, B. A. Richardson, J. Overbaugh, W. R. Morton, R. E. Benveniste, and S. L. Hu.** 1999. Limited breadth of the protective immunity elicited by simian immunodeficiency virus SIVmne gp160 vaccines in a combination immunization regimen. J. Virol. **73**:618–630.
43. **Reeves, J. D., and R. W. Doms.** 2002. Human immunodeficiency virus type 2. J. Gen. Virol. **83**:1253–1265.
44. **Reitter, J. N., R. E. Means, and R. C. Desrosiers.** 1998. A role for carbohydrates in immune evasion in AIDS. Nat. Med. **4**:679–684.
45. **Robinson, H. L., D. C. Montefiori, R. P. Johnson, K. H. Manson, M. L. Kalish, J. D. Lifson, T. A. Rizvi, S. Lu, S. L. Hu, G. P. Mazzara, D. L. Panicali, J. G. Herndon, R. Glickman, M. A. Candido, S. L. Lydy, M. S. Wyand, and H. M. McClure.** 1999. Neutralizing antibody-independent containment of immunodeficiency virus challenges by DNA priming and recombinant pox virus booster immunizations. Nat. Med. **5**:526–534.
46. **Rose, N. F., P. A. Marx, A. Luckay, D. F. Nixon, W. J. Moretto, S. M. Donahoe, D. Montefiori, A. Roberts, L. Buonocore, and J. K. Rose.** 2001. An effective AIDS vaccine based on live attenuated vesicular stomatitis virus recombinants. Cell **106**:539–549.
47. **Stebbing, J., B. Gazzard, and D. C. Douek.** 2004. Where does HIV live? N. Engl. J. Med. **350**:1872–1880.
48. **Sugimoto, C., K. Tadakuma, I. Otani, T. Moritoyo, H. Akari, F. Ono, Y. Yoshikawa, T. Sata, S. Izumo, and K. Mori.** 2003. *nef* gene is required for robust productive infection by simian immunodeficiency virus of T-cell-rich paracortex in lymph nodes. J. Virol. **77**:4169–4180.
49. **Villinger, F., A. E. Mayne, P. Bostik, K. Mori, P. E. Jensen, R. Ahmed, and A. A. Ansari.** 2003. Evidence for antibody-mediated enhancement of simian immunodeficiency virus (SIV) Gag antigen processing and cross presentation in SIV-infected rhesus macaques. J. Virol. **77**:10–24.
50. **Watanabe, M. E.** 2003. Skeptical scientists skewer VaxGen statistics. Nat. Med. **9**:376.
51. **Wei, X., J. M. Decker, S. Wang, H. Hui, J. C. Kappes, X. Wu, J. F. Salazar-Gonzalez, M. G. Salazar, J. M. Kilby, M. S. Saag, N. L. Komarova, M. A. Nowak, B. H. Hahn, P. D. Kwong, and G. M. Shaw.** 2003. Antibody neutralization and escape by HIV-1. Nature **422**:307–312.
52. **Yu, D., T. Shioda, A. Kato, M. K. Hasan, Y. Sakai, and Y. Nagai.** 1997. Sendai virus-based expression of HIV-1 gp120: reinforcement by the V(−) version. Genes Cells **2**:457–466.

A *CCR2-V64I* polymorphism affects stability of CCR2A isoform

Emi E. Nakayama, Yuetsu Tanaka,[a] Yoshiyuki Nagai,[b] Aikichi Iwamoto[c] and Tatsuo Shioda

Objective: A valine to isoleucine substitution at position 64 of CCR2 (*CCR2-64I*) is associated with a delay in progression to AIDS in HIV-1-infected individuals. The aim of the present study is to elucidate the molecular mechanism underlying the effect of this allele.

Design: We analysed the effect of the 64I substitution on levels of expression of CCR2A and CCR2B, two CCR2 isoforms produced by alternative splicing.

Methods: Sendai virus vector was used to express CCR2 molecules.

Results: While CCR2B trafficked well to the cell surface, CCR2A, which differs from CCR2B only by the sequence of its C-terminal cytoplasmic tail, was detected predominantly in the cytoplasm. The level of expression of CCR2A-64I was significantly higher than that of CCR2A without the substitution. On the other hand, the 64I substitution did not affect levels of CCR2B expression. Pulse–chase experiments revealed that the 64I substitution increased the half-life of CCR2A in cells. When co-expressed with CCR5, CCR2A-64I interfered more severely with cell surface expression of CCR5 than did wild-type CCR2A. Furthermore, immunoprecipitation experiments showed that CCR2A co-precipitated with an immature form of CCR5.

Conclusion: These results suggest that CCR2A binds to CCR5 in the cytoplasm and down-modulates its surface expression. We propose that the increased ability of CCR2A-64I to down-modulate CCR5 expression might be a possible cause of a delay in HIV-1 disease progression in patients with this allele.

AIDS 2004, **18**:729–738

Keywords: polymorphism, CCR2-64I, CCR2A, CCR5, stability

Introduction

The chemokine receptor CCR2B has been regarded as a minor HIV-1 coreceptor because only a small number of HIV-1 strains has been shown to use CCR2B as an entry coreceptor [1–3]. Nevertheless, a polymorphism in the CCR2 gene, *CCR2-64I*, has been reported to be associated with delayed disease progression in HIV-1 infected individuals in several Caucasian cohorts [4–8]. This polymorphism, a G-to-A transition at position 190, changes CCR2B codon 64 from valine to isoleucine, introducing a conservative amino acid change into the first transmembrane domain. It was unclear why a single amino acid substitution in a minor coreceptor could affect HIV-1 disease progression, as there was no difference in HIV-1 co-receptor activity between the variant CCR2B-64I and CCR2B without the 64I substitution (CCR2B-64V) [9,10]. Furthermore, these studies also excluded the possibility that CCR2B-64I exerts a dominant-negative effect on the expression and activity of CCR5.

From the Research Institute for Microbial diseases, Osaka University, Osaka, the [a]University of the Ryukyus, Okinawa, [b]Toyama Institute of Health, Toyama, and the [c]Institute of Medical Science, University of Tokyo, Tokyo, Japan.

Correspondence to T. Shioda, Department of Viral Infections, Research Institute for Microbial Diseases, Osaka University. 3-1 Yamada-oka, Suita-shi, Osaka 565-0871, Japan.

Received: 5 May 2003; revised: 27 September 2003; accepted: 15 October 2003.

DOI: 10.1097/01.aids.0000111407.02002.15

ISSN 0269-9370 © 2004 Lippincott Williams & Wilkins

It is possible that the *CCR2* polymorphism may be linked to other polymorphisms in genes that influence AIDS progression. The *CCR2* gene is located approximately 15 kb from the 5′ end of the *CCR5* gene, and the *CCR2-64I* allele is indeed linked to a certain *CCR5* promoter haplotype [11]. However, experiments using promoter–reporter fusion constructs showed that the *CCR5* promoter haplotype, which is in a strong linkage disequilibrium with *CCR2-64I*, did not affect transcriptional activity of the *CCR5* promoter [10]. Thus, the mechanism underlying the protective effect of *CCR2-64I* against AIDS progression still remained to be elucidated.

Two alternatively spliced CCR2 isoforms, CCR2A and CCR2B, were reported to be present in freshly isolated human monocyte, THP-1, and MonoMac 6 leukaemia cell lines [12,13]. An open reading frame encoded in the chromosome corresponds to CCR2B, while alternatively spliced transcripts produce CCR2A. The two CCR2 isoforms differ only in their C-terminal cytoplasmic tails (Fig. 1). Therefore, an individual carrying the *CCR2-64I* allele also produces CCR2A molecules with isoleucine at position 64. Although the cytoplasmic tail spans less than one-fifth of the entire CCR2 molecule, this difference caused a drastic alteration in their localization in cells [13]. While CCR2B trafficked well to the cell surface, CCR2A was detected predominantly in the cytoplasm. A progressive truncation study of the C-terminal cytoplasmic tail indicated that a cytoplasmic retention signal(s) was located in the C-terminal cytoplasmic tail [13]. Nevertheless, CCR2A molecules that successfully trafficked to the cell surface could respond to the stimulation of monocyte chemoattractant protein (MCP)-1 in a similar fashion to CCR2B [14].

As none of the previous studies investigated the effect

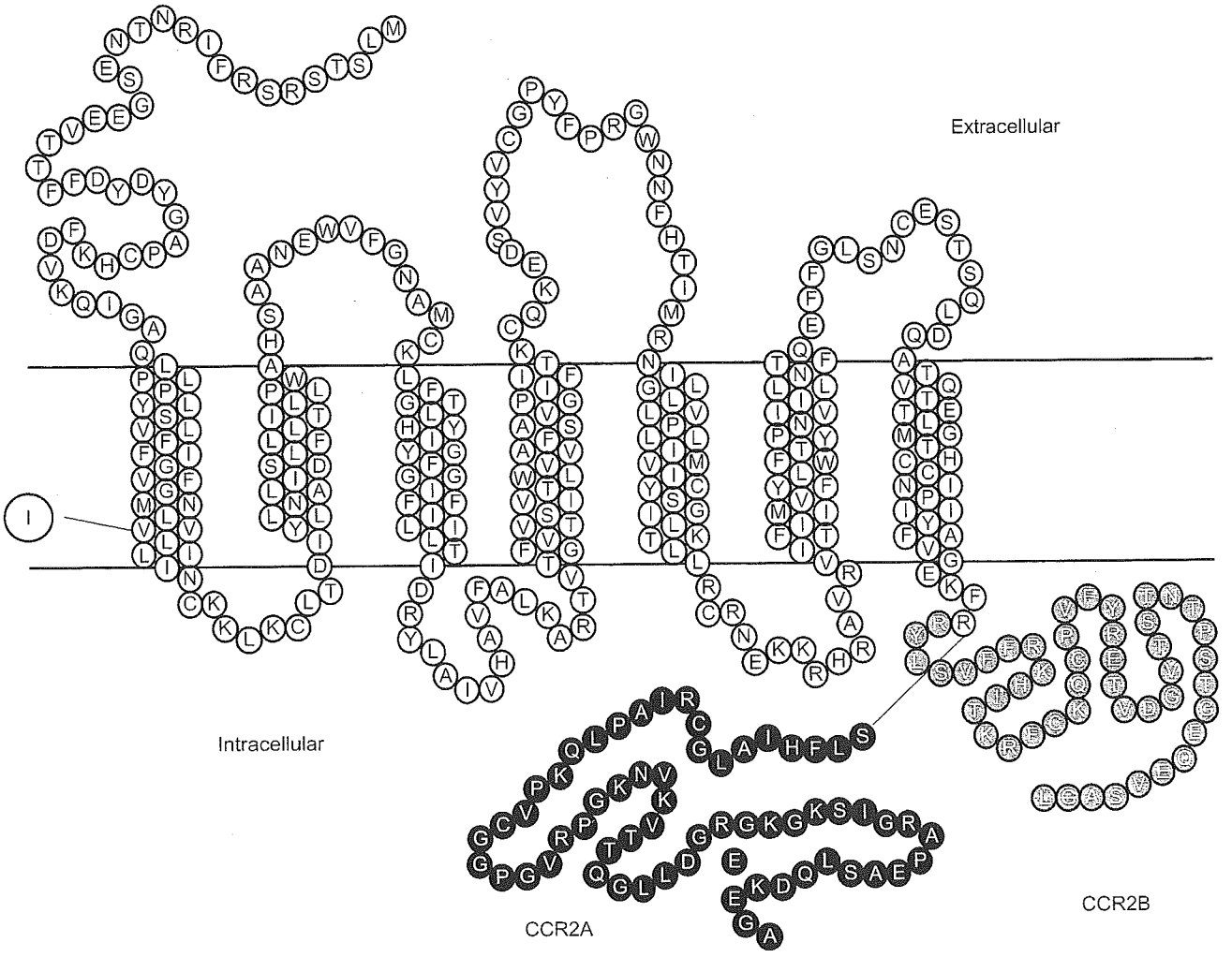

Fig. 1. The structure of the CCR2A and CCR2B molecules. Outlined letters in grey circles denote amino acid residues present in CCR2B. Outlined letters in black circles denote amino acid residues present in CCR2A. A letter I in a large circle denotes a substitution at position 64.

of the 64I substitution on CCR2A molecules, we generated recombinant Sendai viruses (SeV) expressing either CCR2A-64V or CCR2A-64I. Here we show that the 64I substitution indeed affected the stability of CCR2A molecules in cells, and increased the ability of CCR2A to down-modulate the major HIV-1 co-receptor, CCR5.

Materials and methods

Generation of recombinant SeV

THP-1 cells were shown to possess both *CCR2-64V* and *CCR2-64I* alleles by using a standard genotyping method [15]. Therefore, CCR2A-64V, CCR2A-64I, CCR2B-64V, and CCR2B-64I cDNA were obtained by reverse transcription (RT)–PCR from mRNA extracted from THP-1 cells and then inserted to the *Not*I site of pSeV18+b(+). The entire coding regions in the resultant plasmids were verified for sequence authenticity as well as for the presence or absence of the 64I substitution. For generating CCR2A-64V and CCR2A-64I cDNA carrying a c-myc-tag (EQKLI SEEDL) at their C-termini, cloned CCR2A-64V and CCR2A-64I cDNA served as templates for PCR amplification using a primer containing a nucleotide sequence corresponding the c-myc-tag fused with the C-terminal portion of CCR2A. Recombinant SeV carrying CCR2A-64V, CCR2A-64I, CCR2B-64V, CCR2B-64I, or C-myc-tagged versions of CCR2A-64V and CCR2A-64I were recovered according to a previously described method [16]. The wild-type Z strain of SeV served as a control in all the experiments.

Generation of a recombinant vaccinia virus

For generating CCR5 cDNA carrying a HA tag (YPYDVPDYAA) at its C terminus, cloned CCR5 cDNA served as a template for PCR amplification by using a primer containing a haemagglutinin (HA) tag sequence fused with the C-terminal portion of CCR5. The resultant PCR products were then inserted into pNZ68K2-Not. The entire coding region of CCR5-HA was verified for sequence authenticity. A recombinant vaccinia virus (Vac) was recovered from the resultant plasmid according to previously described procedures [17].

Flow cytometric analysis

CV1 monkey kidney cells, U937 monocytic cells and Jurkat T cells were infected with recombinant SeV expressing CCR2A-64V, CCR2A-64I, CCR2B-64V, or CCR2B-64I. Five to 18 h after infection, cells were incubated with MAB150, a mouse monoclonal antibody (MAb) against CCR2 (R & D Systems, Minneapolis, Minnesota, USA). Antibodies bound to cells were detected using fluorescein-5-isothiocyanate (FITC)-conjugated goat antibody directed against mouse IgG (Cappel, Aurora, Ohio, USA). CV1 or H9 cells infected with SeV expressing CCR2A-64V, CCR2A-64I, CCR2B-64V, or CCR2B-64I were superinfected with a recombinant Vac expressing CCR5, CXCR4, or CD4 at 9 h after SeV infection. After incubation for 5 h at 37°C, cells were stained for CCR5 using T227 rat MAb against CCR5 [17] followed by FITC-conjugated goat anti-rat IgG; for CXCR4 using 12G5 mouse MAb (R & D systems) followed by FITC-conjugated goat anti-mouse IgG; or for CD4 using FITC-conjugated anti-human CD4, Leu3a (Becton Dickinson, San Jose, California, USA), and analysed by FACScan (Becton Dickinson).

Immunofluorescence microscopy

CV1 cells expressing CCR2A or CCR2B were fixed and permeabilized before being incubated with MAB150 antibody as described previously [17]. Bound antibodies were then detected using FITC-conjugated goat antibody against mouse IgG. Indirect immunofluorescence was visualized using a Lasersharp2000 Confocal Microscope System (Bio-Rad, Hercules, California, USA). Anti-Calnexin (Stressgen, San Diego, California, USA) or anti-Giantin (CRPinc, Berkeley, California, USA) rabbit polyclonal antibody was used with Cy5-conjugated goat antibody against rabbit IgG (Amersham Pharmacia Biotech, Piscataway, New Jersey, USA).

Chemotaxis assay

Chemotaxis assays were performed according to previously described methods [18]. Briefly, MCP-1 (PeproTech, Rockey Hill, New Jersey, USA) diluted at an indicated concentration of chemotaxis buffer (RPMI 1640 with 0.25% human serum albumin) was added to the bottom chamber of a 5-μm pore polycarbonate Transwell culture insert (Costar; Corning, New York, USA). Jurkat cells were infected with a SeV expressing CCR2A-64V or CCR2A-64I and incubated at 37°C for 4 h. Cells were then washed with RPMI1640 and re-suspended in chemotaxis buffer and added to the upper chamber of the insert. Transmigrated cells in 4 h at 37°C were counted using a FACScan.

Pulse-chase analyses of CCR2A and CCR5

CV1 or U937 cells were infected with a SeV expressing CCR2A-64V-myc or CCR2A-64I-myc. Nine hours after infection, cells were labelled with 500 kbq/ml of EXPRE^{35}S^{35}S[^{35}S] protein labelling mix (> 37 Tbq/mmol; PerkinElmer (Boston, Massachusetts, USA) in amino acid-free medium for 30 min. For CCR5 analysis, cells were infected with a recombinant Vac expressing CCR5-HA, incubated at 37°C for 5 h and then labelled. Cells were then washed, fed with fresh medium and incubated for 0, 15, 30, 60, or 120 min at 37°C, chilled on ice, and lysed in lysis buffer (50 mM Tris–HCl pH7.5, 150 mM NaCl, 1% Nonidet P40, 0.5% sodium deoxycholate). CCR2A

and CCR5 proteins in the lysates were precipitated with anti-myc mouse MAb (9B11; Cell Signaling, Beverly, Massachusetts, USA) and anti-HA high affinity rat MAb (Roche, Indianapolis, Indiana, USA), respectively, using a Protein G Immunoprecipitation Kit (Roche). Precipitated materials were subjected to SDS–PAGE on a 4–12% NuPAGE Bis–Tris gel (Invitrogen, Groningen, Netherlands), and the amount of radiolabel incorporated was visualized on a BAS Imager (Fujix, Kanagawa, Japan).

Gene reporter fusion assay

A recombinant Vac-based gene activation assay using a β-galactosidase gene as a reporter was performed as described previously [19]. Briefly, mouse fibroblast L cells were transfected with β-galactosidase reporter plasmid pGINT7β-gal and infected with a recombinant Vac expressing gp160 of an R5 HIV-1 strain SF162. At the same time, CV1 cells were infected with SeV expressing CCR2A-64V or CCR2A-64I and incubated at 37°C for 9 h. Cells were then superinfected with recombinant Vacs expressing T7 RNA polymerase, human CD4, and CCR5, detached by trypsinization, and cultured at 37°C for 5 h. Then, L and CV-1cells were mixed, incubated for 3 h, and β-galactosidase activities in the cell lysate were measured by using chlorophenol red-β-D-galactopyranoside as substrate.

HIV-1 productive infection

MT4 cells (4×10^5) were infected with SeV expressing CCR2A-64V, CCR2A-64I or parental Z strain of SeV at a multiplicity of infection (MOI) of 40 plaque forming unit (PFU)/cell mixed with SeV expressing CCR5 at an MOI of 10 PFU/cell and incubated at 37°C for 5 h. Cells were then superinfected with 60 ng p24 of an R5 HIV-1 strain SF162. The culture supernatants were collected periodically and p24 levels were measured.

Immunoprecipitation and western blot analysis

CV1 cells were infected with SeV expressing CCR2A-64V-myc or CCR2A-64I-myc, and incubated at 37°C for 9 h. Cells were then superinfected with a Vac expressing CCR5-HA and incubated at 37°C for 5 h and then lysed. CCR2A-64V-myc, CCR2A-64I-myc or CCR5-HA proteins were immunoprecipitated, and subjected to SDS–PAGE as described above. Proteins were then electrophoretically transferred to a PVDF membrane (Immobilon; Millipore, Bedford, Massachusetts, USA). Blots were blocked and probed with the antibodies overnight at 4°C and then incubated with peroxidase-conjugated anti-mouse (Kirkegaard & Perry Laboratories, Gaithersbug, Maryland, USA) or anti-rat IgG (American Qualex, San Clemente, California, USA) and developed using the Immun-Star HRP chemiluminescent kit (Bio-Rad).

Results

Expression of CCR2A and CCR2B

We generated a recombinant SeV expressing either CCR2A-64V or CCR2B-64V. Confocal microscopic observations (Fig. 2a) and flow cytometric analyses (Fig. 2b) confirmed the different subcellular localization of these two CCR2 isoforms. In CCR2B-64V expressing CV1 cells, fluorescent signals of CCR2 were observed mainly on the cell surface. In contrast, CCR2A-64V was localized predominantly to the cytoplasm, although a small portion of CCR2A was observed on the cell surface. In the cytoplasm, signals of an endoplasmic reticulum marker calnexin were only partially co-localized with CCR2A signals (Fig. 2a, left), whereas the majority of signals for the Golgi marker giantin overlapped with those of CCR2A (Fig. 2a, right). These results suggested that most CCR2A molecules were retained in the Golgi.

To assess the effect of the 64I substitution on CCR2A expression, we generated a recombinant SeV expressing CCR2A-64I and compared levels of expression of CCR2A-64I with those of CCR2A-64V. As shown in Fig. 2b, CCR2A-64I showed slightly but significantly higher levels of expression than CCR2A-64V in various cell types, despite the same promoter being used. The mean fluorescence intensity (MFI) of CCR2A-64I and CCR2A-64V was 274 and 140 in CV1, 133 and 40 in U937 monocystic cells, and 29 and 21 in Jurkat T cells. The difference was greater in U937 cells than in Jurkat cells. The difference was also observed at 5, 12, and 18 h after infection of recombinant SeVs (Fig. 2c). Exactly the same result was obtained when recombinant SeV expressing C-myc-tagged versions of CCR2A-64V (CCR2A-64V-myc) and CCR2A-64I (CCR2A-64I-myc) were used (Fig. 2c). In contrast, we failed to detect any difference in the levels of expression between CCR2B-64V and CCR2B-64I (MFI 2698 and 2663, respectively; Fig. 2b), as had been described in the previous reports [9,10]. Northern blot analyses confirmed that there was no difference in the amount of CCR2 mRNA among cells expressing CCR2A-64V, CCR2A-64I, CCR2A-64V-myc, CCR2A-64I-myc, CCR2B-64V and CCR2B-64I (data not shown). These data clearly indicate that the substitution of valine to isoleucine affects levels of cell surface expression of CCR2A, but not of CCR2B.

Chemokine receptor activity of recombinant CCR2A-64V and CCR2A-64I

To determine whether or not CCR2A molecules expressed by a recombinant SeV fully retained chemokine receptor activity, we performed a chemotaxis assay. As shown in Fig. 2d, both cells expressing CCR2A-64V and CCR2A-64I migrate toward MCP-1. However, cells expressing CCR2A-64I migrated

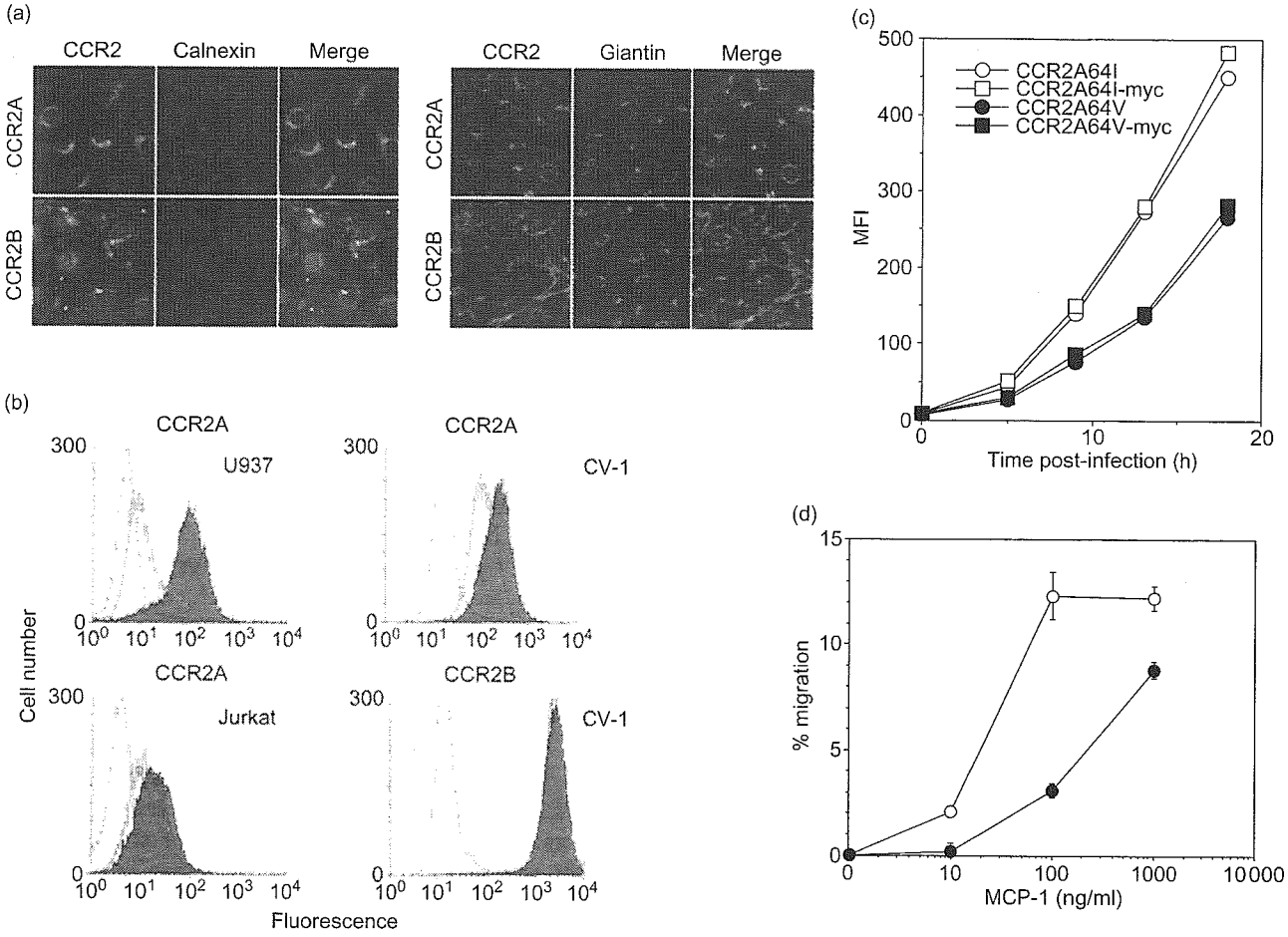

Fig. 2. (a) Subcellular distribution of CCR2A-64V and CCR2B-64V in CV1 cells. SeV vector (SeV) was used to express the CCR2A-64V and CCR2B-64V molecules. Cells were fixed and permeabilized before staining with MAB150 anti-CCR2 mouse MAb followed by FITC-labelled anti-mouse IgG. Cells were then re-stained with anti-calnexin or anti-giantin rabbit polyclonal antibody followed by Cy5-labelled anti-rabbit IgG, and analysed by confocal laser microscopy. (b) Surface expression of CCR2A-64V (green) and CCR2A-64I (red) in U937, CV1 or Jurkat cells. Cells infected with the parental Z strain served as a negative control (black). In lower right panel, green and red indicates CCR2B-64V and CCR2B-64I, respectively. (c) The cell surface expression of CCR2A-64I (open circles), CCR2A-64I-myc (open squares), CCR2A-64V (filled circles), and CCR2A-64V-myc (filled squares) at 5, 9, 12 and 18 h after infection by SeV. MFI indicates mean fluorescence intensity of each sample. (d) Chemokine receptor activity of recombinant CCR2A-64V and CCR2A-64I. Jurkat cells infected with SeV expressing CCR2A-64V (closed circles) or CCR2A-64I (open circles) migrated in response to increasing concentration of MCP-1. Data points are means of triplicate determination with standard deviations.

more efficiently than those expressing CCR2A-64V. These results are in good agreement with the observation that expression of CCR2A-64I is higher than that of CCR2A-64V.

CCR2A-64I is more stable than CCR2A-64V

Differential levels of expression between CCR2A-64V and CCR2A-64I prompted us to compare the rate of degradation of those proteins in pulse–chase experiments. For this purpose, we used recombinant SeV expressing CCR2A-64V-myc or CCR2A-64I-myc. Comparison of immunoprecipitated materials from ^{35}S-labelled CV1 cells expressing CCR2A-64V-myc and CCR2A-64I-myc showed that almost identical levels of CCR2A-64V-myc and CCR2A-64I-myc proteins were synthesized during the 30-min labelling period (t = 0) (Fig. 3a). However, CCR2A-64V-myc proteins appeared to degrade more rapidly than CCR2A-64I-myc proteins. The half-life of CCR2A-64I-myc was approximately 90 min, whereas that of CCR2A-64V-myc was approximately 50 min in CV1 cells (Fig. 3b). More prominent results were obtained when we used U937 cells, as the half-life of CCR2A-64I-myc was approximately 60 min, whereas that of CCR2A-64V-myc was approximately 18 min in U937 cells. This finding is in a good agreement with the observation

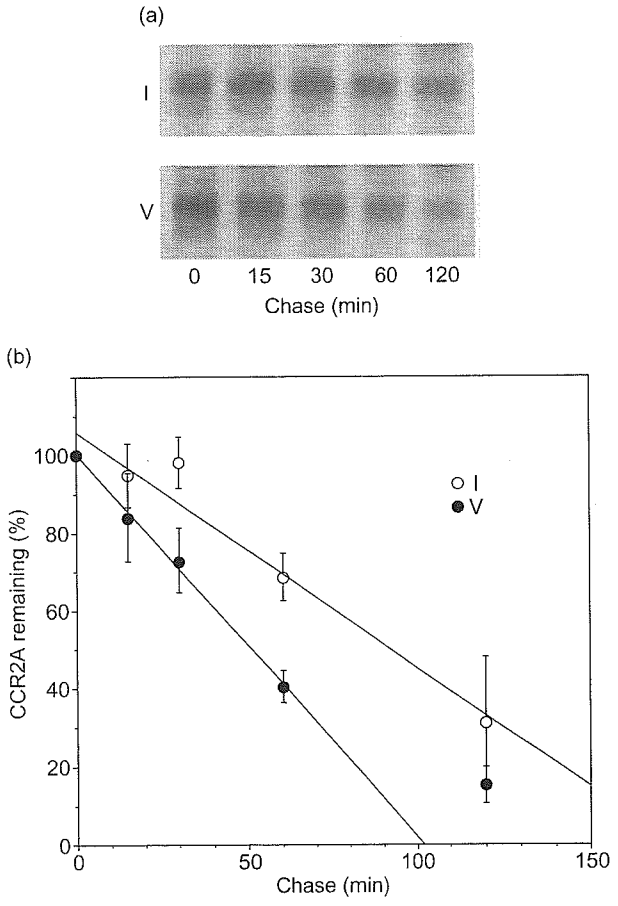

Fig. 3. CCR2A-64I is more stable than CCR2A-64V. CV1 cells were infected with SeV expressing CCR2A-64V-myc and CCR2A-64I-myc for 9 h. Cells were labelled for 30 min and then harvested following the chase time indicated. (a) Representative gels of pulse–chase analysis. (b) Phosphorlmager analysis of the gels shown in (a). Open and closed circles denote cells infected with SeV expressing CCR2A-64V-myc and CCR2A-64I-myc, respectively. Data points are means of four independent experiments with standard deviations.

that the difference in cell surface expression levels between CCR2A-64V and CCR2A-64I was greater in U937 cells than in CV-1 cells (Fig. 2b). These results indicate that higher cell surface expression of CCR2A-64I was due to increased stability of CCR2A-64I. On the other hand, we failed to detect any significant difference in the half-life between CCR2B-64V and CCR2B-64I (data not shown).

CCR5 but not CXCR4 expression was more severely blocked by co-expression of CCR2A-64I than by co-expression of CCR2A-64V

To determine whether or not CCR2A has a dominant-negative effect on the expression of major HIV-1 receptor molecules, we first inoculated SeV expressing CCR2A-64V or CCR2A-64I in CV1 cells and incubated the cells for 9 h at 37°C. The cells were then superinfected with recombinant Vac expressing CCR5, CXCR4, or CD4. Five hours after Vac infection, surface expression of CCR5, CXCR4, or CD4 were examined by flow cytometry. As shown in Fig. 4a, the CCR5 MFI of cells co-infected with parental Z strain of SeV was 391, while that of the cells co-infected with SeV expressing CCR2A-64V was 297, indicating that co-expression of CCR2A-64V significantly reduced levels of CCR5 expression on the cell surface. This dominant-negative effect on CCR5 expression was more prominent when SeV expressing CCR2A-64I were used (MFI, 145) than SeV expressing CCR2A-64V were used. The same results were obtained when we used recombinant SeV expressing CCR2A-64V-myc and CCR2A-64I-myc (MFI, 300 and 179, respectively). Similar results were obtained when CV1 cells were inoculated with Vac expressing CCR5 5 h after infection by SeV expressing CCR2A, as the CCR5 MFI on cells co-infected with Z, SeV expressing CCR2A-64V, and Sev expressing CCR2A-64I, was 299, 205, and 160, respectively. Furthermore, the dominant-negative effect of CCR2A on CCR5 expression was also observed when T cell line H9 was used. The CCR5 MFI on H9 cells co-infected with Z, SeV expressing CCR2A-64V, and SeV expressing CCR2A-64I was 263, 230 and 195, respectively. In contrast, the cell surface expression of CXCR4, another major co-receptor, as well as that of CD4, the main receptor of HIV-1, were not affected by CCR2A-64V or CCR2A-64I (Fig. 4a). In contrast with CCR2A, neither CCR2B-64V nor CCR2B-64I affected the surface expression of CCR5 (Fig. 4b).

HIV-1 coreceptor activity of CCR5 was more dramatically reduced by co-expression of CCR2A-64I than by co-expression of CCR2A-64V

To assess the effect of CCR2A-64I on HIV-1 infection, we examined the ability of cells expressing both CCR2A and CCR5 molecules to support CD4-dependent cell fusion mediated by an HIV-1 envelope protein of the R5 strain SF162. For this purpose, we prepared CV1 cells expressing both CCR5 and CCR2A as described in Fig. 4a, and mixed those cells with mouse L cells expressing HIV-1 envelope protein. As shown in Fig. 5a, the envelope-mediated cell fusion activity of CCR5 was more dramatically reduced by co-expression of CCR2A-64I than by that of CCR2A-64V.

We also inoculated a live SF162 strain of HIV-1 into CD4 positive MT4 cells expressing both CCR5 and CCR2A. As shown in Fig. 5b, MT4 cells expressing CCR5 and CCR2A-64V supported SF162 replication better than those expressing CCR5 and CCR2A-64I.

Co-immunoprecipitation of CCR2A and CCR5

Many seven-transmembrane receptors, including che-

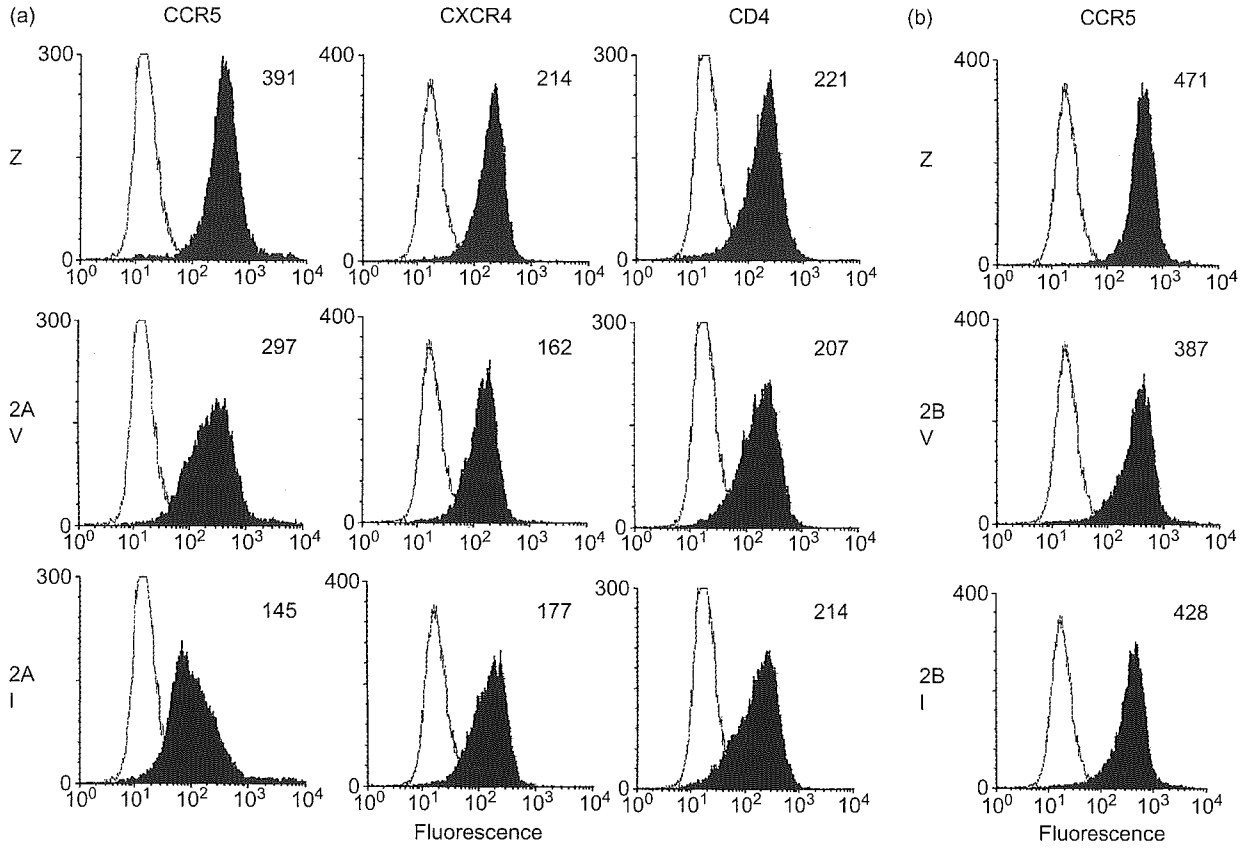

Fig. 4. (a) Effect of CCR2A-64V and CCR2A-64I on HIV-1 corecepter expression. Vac vectors were used to express CCR5, CXCR4 and CD4 in the CV1 cells inoculated with SeV expressing CCR2A-64V or CCR2A-64I. Z denotes the wild-type SeV. Five hours after infection, cells were stained with MAb against CCR5, CXCR4, or CD4. Flow cytometry was used to determine surface expression levels. The number in each panel indicates mean fluorescence intensity. (b) Effect of CCR2B-64V and CCR2B-64I on CCR5 expression.

mokine receptors, have been reported to form homo-oligomers. CCR2A is highly homologous to CCR5 (68% at the amino acid level), and formation of heterodimers between CCR2B and CCR5 was reported previously [20]. The dominant-negative effect of CCR2A on CCR5 expression shown in Figs 4a, 5a and 5b raised the possibility of heterodimer formation between CCR2A and CCR5. To test this hypothesis, we used SeV expressing CCR2A-64V-myc or CCR2A-64I-myc, and Vac expressing HA-tagged version of CCR5 (CCR5-HA). Anti-myc and anti-HA immunoprecipitates from cell lysates were developed in Western blots by using anti-HA or anti-myc antibodies. As expected, CCR5-HA was detected by anti-HA antibody in anti-myc-derived immunoprecipitates from CCR5-HA and CCR2A-64V-myc co-expressed cell lysates as well as from CCR5-HA and CCR2A-64I-myc co-expressed cell lysates. At the same time, CCR2A-64V-myc and CCR2A-64I-myc were detected by anti-myc antibody in anti-HA-derived immunoprecipitates of CCR5-HA and CCR2A-64V-myc co-expressed cell lysates and in that of CCR5-HA and CCR2A-64I-myc co-expressed cell lysates (Fig. 5c). These results clearly indicate that CCR2A formed heterodimers with CCR5.

In CCR5-HA expressing cells, we consistently observed two types of CCR5-HA molecules with different electrophoretic mobility. When we used anti-HA antibody to precipitate CCR5-HA directly, most of the CCR5-HA molecules migrated at approximately 38 kDa. In contrast, most of the CCR5-HA molecules that co-precipitated with CCR2A-64V-myc or CCR2A-64I-myc migrated at 37 kDa. We speculated that the CCR5-HA of 38 kDa represented authentic CCR5 molecules and that of 37 kDa represented immature forms of CCR5. To verify the maturation process of CCR5, we labelled the cells infected with Vac expressing CCR5-HA by [^{35}S]-methionine for 30 min and harvested those cells following chase periods ranging from 15 to 60 min. As shown in Fig. 5d, the 37-kDa CCR5-HA could be detected only after the labelling period (0 min). This result suggests that CCR2A binds to premature forms of CCR5 and

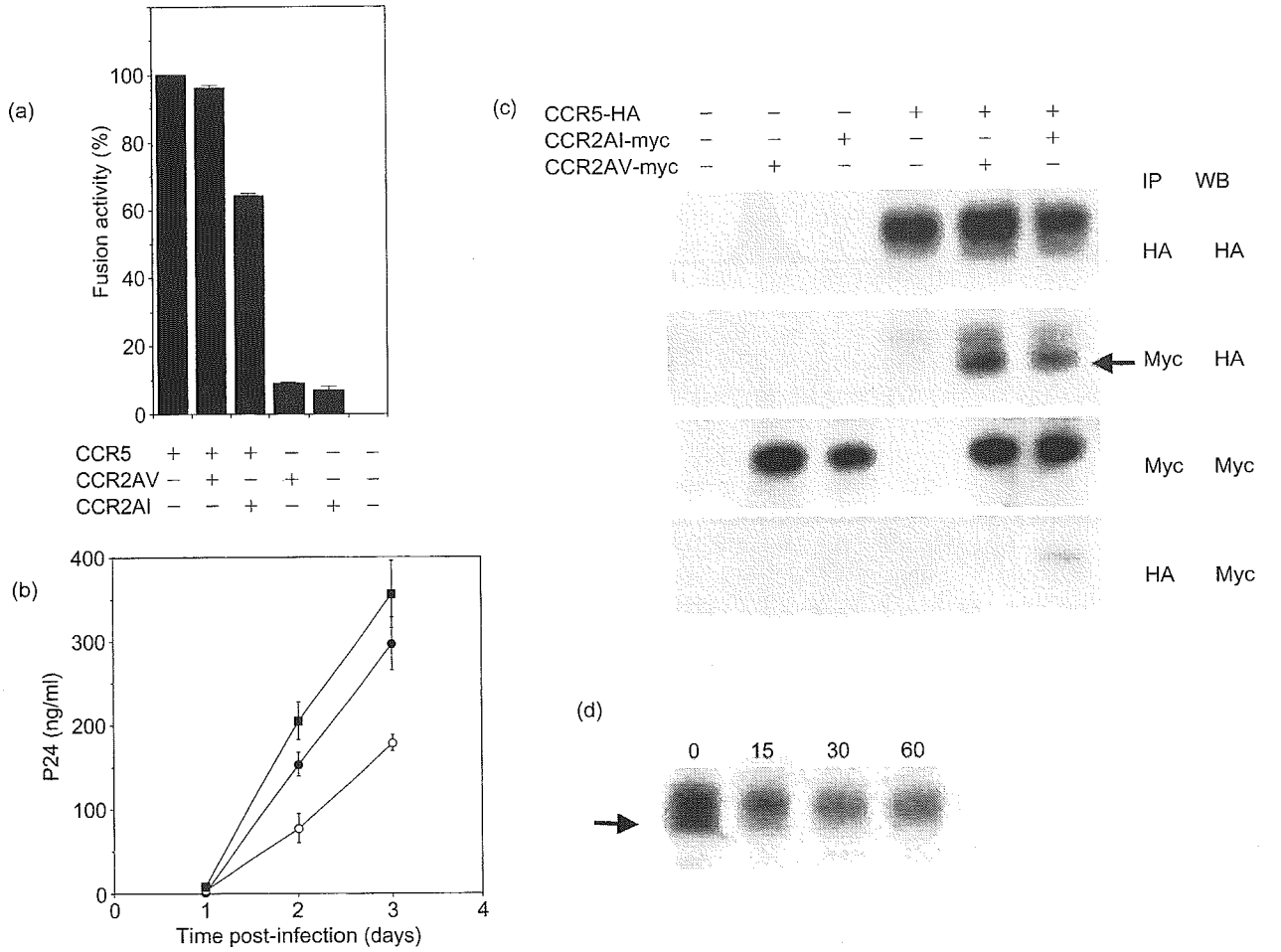

Fig. 5. (a) Coreceptor activity of CCR5 in CCR2A-64V or CCR2A-64I co-expressed cells. SeV vector was used to express CCR2A-64V or CCR2A-64I, and Vac vector was used to express CCR5 as described in Fig. 4. HIV-1 coreceptor activity of each sample was measured using the method described in Materials and methods. The wild-type Vac WR strain was used as a CCR5-negative control, and the wild-type SeV Z strain was used as the CCR2A-negative control. (b) MT4 cells were co-infected with SeV expressing CCR5 and SeV expressing CCR2A-64V (filled circles), CCR2A-64I (open circles), or parental Z strain (filled squares). Five hours after infection, cells were inoculated with an HIV-1 strain SF162. (c) Co-immunopresipitation of CCR2A and CCR5. Recombinant Vac expressing CCR5-HA or parental WR strain (−) was superinfected in CV1 cells infected with SeVs expressing CCR2A-64V-myc, CCR2A-64I-myc, or the parental Z strain (−). Immunoprecipitation and Western blot analysis were performed by using anti-HA or anti-myc antibody. An arrow indicates 37-kDa CCR5-HA molecules. (d) Pulse–chase analysis of CCR5 molecules. A recombinant Vac expressing CCR5-HA was inoculated into CV1 cells. An arrow indicates 37-kDa CCR5-HA molecules.

interferes with the maturation process of CCR5 molecules in cytoplasm.

Discussion

Many independent cohort studies have affirmed the AIDS-delaying effects of the *CCR2-64I* allele [4–8], but the molecular mechanism of this protective effect had not yet been elucidated. In the present study, we demonstrated that a valine to isoleucine substitution at position 64 increased stability of CCR2A but not of CCR2B molecules in cells. When co-expressed with the major HIV-1 co-receptor CCR5, CCR2A-64I more severely interfered with cell surface expression as well as HIV-1 co-receptor activity of CCR5 than CCR2A-64V. Furthermore, CCR2A was shown to co-precipitate with immature form of CCR5. These results suggest that CCR2A binds to CCR5 in the cytoplasm and dominantly interferes with CCR5 maturation and surface expression. On the other hand, the 64I substitution did not affect the level of CCR2B expression, being consistent with results published previously [9,10]. We speculate that increased ability of CCR2A-64I to down modulate CCR5 expression

might be a possible cause of delay in HIV-1 disease progression in patients with this allele. Alternatively, it is also possible that immune cell trafficking and/or signalling might be affected by CCR2A stabilization, leading to a delay in HIV-1 diseases.

Previously, Mellado *et al.* reported that CXCR4 could dimerize with CCR2B-64I variants but not with wild-type CCR2B-64V upon stimulation with SDF-1 and MCP-1. Based on this finding, they proposed that this ability of CCR2B-64I to heterodimerize with CXCR4 may cause a delay in AIDS progression [20]. However, several independent cohort studies have shown that the effects of the *CCR2-64I* allele were more pronounced in earlier stages of disease than in latter stages [5,8,21]. In a Dutch cohort, delay in HIV-1 disease progression was more pronounced before the emergence of X4 variants and was not observed after the emergence of X4 variants in individuals with the CCR2-64I allele [6]. Therefore, it is unlikely that CCR2B-64I/CXCR4 heterodimerization is the main cause of delay in AIDS progression in individuals with CCR2-64I.

Previous studies exploring the oligomerization of chemokine receptors also yielded controversial results. Rodrigues-Frade *et al.* reported that CCR2B forms homodimers upon stimulation by MCP-1 [22]. Other studies, however, have shown that CCR5 [23,24] and CXCR4 [25] can form homodimers without any stimulation by their ligands. Although we did not test whether or not stimulation with MCP-1 and/or RANTES increases hetero-oligomer formation between CCR2A and CCR5, our present results support the latter model that chemokine receptors may form oligomers without stimulation by their ligands.

In addition to AIDS pathogenesis, the CCR2-64I allele was reported to be associated with lower risks of coronary artery calcification [26] and acute rejection in renal transplantation [27]. Our present results shed light onto possible mechanisms of the association of this allele with such diverse human phenotypes. It is now widely accepted that monocyte attachment to cardiovascular wall is the first event implicated in atherogenesis of coronary arteries [28,29]. Since monocytes are known to express both CCR2A and CCR2B [13], an increased stability of CCR2A resulting from the 64I substitution may interfere with the function of CCR2B in monocytes, leading to decreased monocyte invasion to cardiovascular walls. With respect to acute rejection in renal transplantation, CCR5 is known to play an important role in both rejection of renal transplantation [30] and experimental graft-versus-host disease models [31]. Therefore, it is possible that an increased ability of CCR2A-64I to interfere with CCR5 expression can cause a decreased frequency of acute rejection after renal transplantation in recipients with this allele.

Previous studies have failed to show a statistically significant difference in levels of CCR5 expression on stimulated or non-stimulated peripheral blood mononuclear cells between CCR2-64I homozygotes and CCR2-64V homozygotes [9,10,32], although a slight reduction was noted in CCR2-64I homozygotes. In fact, we also failed to observe a statistically significant reduction of CCR5 levels on peripheral CD4 cells of homozygotes of CCR2-64I (data not shown). CCR2 is reported to be expressed on monocytes/macrophages [33], basophils [34,35], B cells [36], NK cells [37], dendritic cells [38,39], and a limited population of T cells [40]. Although we observed very few CCR2 cells in peripheral blood mononuclear cells, Bartoli *et al.* reported that numerous mononuclear cells in tonsil expressed CCR2A [41]. It may be possible that specific cell types expressing both CCR2A and CCR5 in tonsil or lymph nodes play an important role in AIDS pathogenesis and are responsible for the delay in HIV-1 diseases observed in patients with CCR2-64I.

Acknowledgements

pGIT7 beta-gal was kindly supplied by E. Berger. We thank D. Chao for critical discussion and S. Bando for technical assistance.

Sponsorship: Supported by grants from the Human Science Foundation, the Ministry of Education, Culture, Sports, Science, and Technology, and the Ministry of Health, Labour and Welfare, Japan.

References

1. Doranz BJ, Rucker J, Yi Y, Smyth RJ, Samson M, Peiper SC, *et al.* **A dual-tropic primary HIV-1 isolate that uses fusin and the beta-chemokine receptors CKR-5, CKR-3, and CKR-2b as fusion cofactors.** *Cell* 1996, **85**:1149–1158.
2. Rucker J, Edinger AL, Sharron M, Samson M, Lee B, Berson JF, *et al.* **Utilization of chemokine receptors, orphan receptors, and herpesvirus- encoded receptors by diverse human and simian immunodeficiency viruses.** *J Virol* 1997, **71**:8999–9007.
3. Penton-Rol G, Cota M, Polentarutti N, Luini W, Bernasconi S, Borsatti A, *et al.* **Up-regulation of CCR2 chemokine receptor expression and increased susceptibility to the multitropic HIV strain 89.6 in monocytes exposed to glucocorticoid hormones.** *J Immunol* 1999, **163**:3524–3529.
4. Smith MW, Dean M, Carrington M, Winkler C, Huttley GA, Lomb DA, *et al.* **Contrasting genetic influence of CCR2 and CCR5 variants on HIV-1 infection and disease progression. Hemophilia Growth and Development Study (HGDS), Multicenter AIDS Cohort Study (MACS), Multicenter Hemophilia Cohort Study (MHCS), San Francisco City Cohort (SFCC), ALIVE Study.** *Science* 1997, **277**:959–965.
5. Kostrikis LG, Huang Y, Moore JP, Wolinsky SM, Zhang L, Guo Y, *et al.* **A chemokine receptor CCR2 allele delays HIV-1 disease progression and is associated with a CCR5 promoter mutation.** *Nat Med* 1998, **4**:350–353.
6. van Rij RP, de Roda Husman AM, Brouwer M, Goudsmit J, Coutinho RA, Schuitemaker H. **Role of CCR2 genotype in the clinical course of syncytium-inducing (SI) or non-SI human immunodeficiency virus type 1 infection and in the time to**

conversion to SI virus variants. *J Infect Dis* 1998, **178**: 1806–1811.
7. Ioannidis JP, Rosenberg PS, Goedert JJ, Ashton LJ, Benfield TL, Buchbinder SP, *et al.* **Effects of CCR5-Delta32, CCR2-64I, and SDF-1 3'A alleles on HIV-1 disease progression: An international meta-analysis of individual- patient data.** *Ann Intern Med* 2001, **135**:782–795.
8. Mulherin SA, O'Brien TR, Ioannidis JP, Goedert JJ, Buchbinder SP, Coutinho RA, *et al.* **Effects of CCR5-Delta32 and CCR2-64I alleles on HIV-1 disease progression: the protection varies with duration of infection.** *AIDS* 2003, **17**:377–387.
9. Lee B, Doranz BJ, Rana S, Yi Y, Mellado M, Frade JM, *et al.* **Influence of the CCR2-V64I polymorphism on human immunodeficiency virus type 1 coreceptor activity and on chemokine receptor function of CCR2b, CCR3, CCR5, and CXCR4.** *J Virol* 1998, **72**:7450–7458.
10. Mariani R, Wong S, Mulder LC, Wilkinson DA, Reinhart AL, LaRosa G, *et al.* **CCR2-64I polymorphism is not associated with altered CCR5 expression or coreceptor function.** *J Virol* 1999, **73**:2450–2459.
11. Mummidi S, Ahuja SS, Gonzalez E, Anderson SA, Santiago EN, Stephan KT, *et al.* **Genealogy of the CCR5 locus and chemokine system gene variants associated with altered rates of HIV-1 disease progression.** *Nat Med* 1998, **4**: 786–793.
12. Charo IF, Myers SJ, Herman A, Franci C, Connolly AJ, Coughlin SR. **Molecular cloning and functional expression of two monocyte chemoattractant protein 1 receptors reveals alternative splicing of the carboxyl-terminal tails.** *Proc Natl Acad Sci USA* 1994, **91**:2752–2756.
13. Wong LM, Myers SJ, Tsou CL, Gosling J, Arai H, Charo IF. **Organization and differential expression of the human monocyte chemoattractant protein 1 receptor gene. Evidence for the role of the carboxyl-terminal tail in receptor trafficking.** *J Biol Chem* 1997, **272**:1038–1045.
14. Sanders SK, Crean SM, Boxer PA, Kellner D, LaRosa GJ, Hunt SW, 3rd. **Functional differences between monocyte chemotactic protein-1 receptor A and monocyte chemotactic protein-1 receptor B expressed in a Jurkat T cell.** *J Immunol* 2000, **165**:4877–4883.
15. Louisirirotchanakul S, Liu H, Roongpisuthipong A, Nakayama EE, Takebe Y, Shioda T, *et al.* **Genetic analysis of HIV-1 discordant couples in Thailand: association of CCR2 64I homozygosity with HIV-1-negative status.** *J Acquir Immune Defic Syndr* 2002, **29**:314–315.
16. Kato A, Sakai Y, Shioda T, Kondo T, Nakanishi M, Nagai Y. **Initiation of Sendai virus multiplication from transfected cDNA or RNA with negative or positive sense.** *Genes Cells* 1996, **1**:569–579.
17. Shioda T, Nakayama EE, Tanaka Y, Xin X, Liu H, Kawana-Tachikawa A, *et al.* **Naturally occurring deletional mutation in the C-terminal cytoplasmic tail of CCR5 affects surface trafficking of CCR5.** *J Virol* 2001, **75**:3462–3468.
18. Shioda T, Kato H, Ohnishi Y, Tashiro K, Ikegawa M, Nakayama EE, *et al.* **Anti-HIV-1 and chemotactic activities of human stromal cell-derived factor 1alpha (SDF-1alpha) and SDF-1beta are abolished by CD26/dipeptidyl peptidase IV-mediated cleavage.** *Proc Natl Acad Sci USA* 1998, **95**:6331–6336.
19. Nakayama EE, Shioda T, Tatsumi M, Xin X, Yu D, Ohgimoto S, *et al.* **Importance of the N-glycan in the V3 loop of HIV-1 envelope protein for CXCR-4- but not CCR-5-dependent fusion.** *FEBS Lett* 1998, **426**:367–372.
20. Mellado M, Rodriguez-Frade JM, Vila-Coro AJ, de Ana AM, Martinez AC. **Chemokine control of HIV-1 infection.** *Nature* 1999, **400**:723–724.
21. Michael NL, Louie LG, Rohrbaugh AL, Schultz KA, Dayhoff DE, Wang CE, *et al.* **The role of CCR5 and CCR2 polymorphisms in HIV-1 transmission and disease progression.** *Nat Med* 1997, **3**:1160–1162.
22. Rodriguez-Frade JM, Vila-Coro AJ, de Ana AM, Albar JP, Martinez AC, Mellado M. **The chemokine monocyte chemoattractant protein-1 induces functional responses through dimerization of its receptor CCR2.** *Proc Natl Acad Sci USA* 1999, **96**: 3628–3633.
23. Benkirane M, Jin DY, Chun RF, Koup RA, Jeang KT. **Mechanism of transdominant inhibition of CCR5-mediated HIV-1 infection by ccr5delta32.** *J Biol Chem* 1997, **272**:30603–30606.
24. Issafras H, Angers S, Bulenger S, Blanpain C, Parmentier M, Labbe-Jullie C, *et al.* **Constitutive agonist-independent CCR5 oligomerization and antibody- mediated clustering occurring at physiological levels of receptors.** *J Biol Chem* 2002, **277**: 34666–34673.
25. Babcock GJ, Farzan M, Sodroski J. **Ligand-independent dimerization of CXCR4, a principal HIV-1 coreceptor.** *J Biol Chem* 2003, **278**:3378–3385.
26. Valdes AM, Wolfe ML, O'Brien EJ, Spurr NK, Gefter W, Rut. A, *et al.* **Val64Ile polymorphism in the C-C chemokine receptor 2 is associated with reduced coronary artery calcification.** *Arterioscler Thromb Vasc Biol* 2002, **22**:1924–1928.
27. Abdi R, Tran TB, Sahagun-Ruiz A, Murphy PM, Brenner BM, Milford EL, *et al.* **Chemokine receptor polymorphism and risk of acute rejection in human renal transplantation.** *J Am Soc Nephrol* 2002, **13**:754–758.
28. Ross R. **The pathogenesis of atherosclerosis: a perspective for the 1990s.** *Nature* 1993, **362**:801–809.
29. Hanke H, Lenz C, Finking G. **The discovery of the pathophysiological aspects of atherosclerosis–a review.** *Acta Chir Belg* 2001, **101**:162–169.
30. Segerer S, Cui Y, Eitner F, Goodpaster T, Hudkins KL, Mack M, *et al.* **Expression of chemokines and chemokine receptors during human renal transplant rejection.** *Am J Kidney Dis* 2001, **37**:518–531.
31. Murai M, Yoneyama H, Harada A, Yi Z, Vestergaard C, Guo B, *et al.* **Active participation of CCR5(+)CD8(+) T lymphocytes in the pathogenesis of liver injury in graft-versus-host disease.** *J Clin Invest* 1999,104:49-57.
32. Shieh B, Liau YE, Hsieh PS, Yan YP, Wang ST, Li C. **Influence of nucleotide polymorphisms in the CCR2 gene and the CCR5 promoter on the expression of cell surface CCR5 and CXCR4.** *Int Immunol* 2000, **12**:1311–1318.
33. Fantuzzi L, Borghi P, Ciolli V, Pavlakis G, Belardelli F, Gessani S. **Loss of CCR2 expression and functional response to monocyte chemotactic protein (MCP-1) during the differentiation of human monocytes: role of secreted MCP-1 in the regulation of the chemotactic response.** *Blood* 1999, **94**:875–883.
34. Ochensberger B, Tassera L, Bifrare D, Rihs S, Dahinden CA. **Regulation of cytokine expression and leukotriene formation in human basophils by growth factors, chemokines and chemotactic agonists.** Eur *J Immunol* 1999, **29**:11–22.
35. Iikura M, Miyamasu M, Yamaguchi M, Kawasaki H, Matsushima K, Kitaura M, *et al.* **Chemokine receptors in human basophils: inducible expression of functional CXCR4.** *J Leukoc Biol* 2001, **70**:113–120.
36. Frade JM, Mellado M, del Real G, Gutierrez-Ramos JC, Lind P, Martinez AC. **Characterization of the CCR2 chemokine receptor: functional CCR2 receptor expression in B cells.** *J Immunol* 1997, **159**:5576–5584.
37. Polentarutti N, Allavena P, Bianchi G, Giardina G, Basile A, Sozzani S, *et al.* **IL-2-regulated expression of the monocyte chemotactic protein-1 receptor (CCR2) in human NK cells: characterization of a predominant 3.4-kilobase transcript containing CCR2B and CCR2A sequences.** *J Immunol* 1997, **158**:2689–2694.
38. Sallusto F, Schaerli P, Loetscher P, Schaniel C, Lenig D, Mackay CR, *et al.* **Rapid and coordinated switch in chemokine receptor expression during dendritic cell maturation.** Eur *J Immunol* 1998, **28**:2760–2769.
39. Vanbervliet B, Homey B, Durand I, Massacrier C, Ait-Yahia S, de Bouteiller O, *et al.* **Sequential involvement of CCR2 and CCR6 ligands for immature dendritic cell recruitment: possible role at inflamed epithelial surfaces.** Eur *J Immunol* 2002, **32**:231–242.
40. Rabin RL, Park MK, Liao F, Swofford R, Stephany D, Farber JM. **Chemokine receptor responses on T cells are achieved through regulation of both receptor expression and signaling.** *J Immunol* 1999, **162**:3840–3850.
41. Bartoli C, Civatte M, Pellissier JF, Figarella-Branger D. **CCR2A and CCR2B, the two isoforms of the monocyte chemoattractant protein-1 receptor are up-regulated and expressed by different cell subsets in idiopathic inflammatory myopathies.** *Acta Neuropathol (Berl)* 2001, **102**:385–392.

JOURNAL OF VIROLOGY, Apr. 2003, p. 4060–4069
0022-538X/03/$08.00+0 DOI: 10.1128/JVI.77.7.4060–4069.2003

Vol. 77, No. 7

Possible Role of Dimerization in Human Immunodeficiency Virus Type 1 Genome RNA Packaging

Jun-Ichi Sakuragi,[1]* Shigeharu Ueda,[2] Aikichi Iwamoto,[3] and Tatsuo Shioda[1]

Department of Viral Infections[1] and Department of Neurovirology,[2] Research Institute for Microbial Diseases, Osaka University, Suita, Osaka 565, and Division of Infectious Diseases, Advanced Clinical Research Center, Institute of Medical Science, University of Tokyo, Minato-ku, Tokyo 108-8639,[3] Japan

Received 25 July 2002/Accepted 20 December 2002

The dimer initiation site/dimer linkage sequence (DIS/DLS) region in the human immunodeficiency virus type 1 (HIV-1) RNA genome is suggested to play important roles in various steps of the virus life cycle. However, due to the presence of a putative DIS/DLS region located within the encapsidation signal region (E/psi), it is difficult to perform a mutational analysis of DIS/DLS without affecting the packaging of RNA into virions. Recently, we demonstrated that duplication of the DIS/DLS region in viral RNA caused the production of partially monomeric RNAs in virions, indicating that the region indeed mediated RNA-RNA interaction. We utilized this system to assess the precise location of DIS/DLS in the 5′ region of the HIV-1 genome with minimum effect on RNA packaging. We found that the entire lower stem of the U5/L stem-loop was required for packaging, whereas the region important for dimer formation was only 10 bases long within the lower stem of the U5/L stem-loop. The R/U5 stem-loop was required for RNA packaging but was completely dispensable for dimer formation. The SL1 lower stem was important for both dimerization and packaging, but surprisingly, deletion of the palindromic sequence at the top of the loop only partially affected dimerization. These results clearly indicated that the E/psi of HIV-1 is much larger than the DIS/DLS and that the primary DIS/DLS is completely included in the E/psi. Therefore, it is suggested that RNA dimerization is a part of RNA packaging, which requires multiple steps.

Retrovirus particles contain single-stranded positive-sense RNA as the genome. The genomic RNA always forms dimers in mature virions. These two RNA molecules are noncovalently linked, since incubation at high temperature (~70°C) or treatment with denaturing agents, such as formamide, easily dissociates them (for a review, see references 10 and 19). Electron microscopic observation revealed that the two RNA molecules are linked symmetrically and the contact point of the dimer, called the dimer linkage sequence (DLS), is located near the 5′ end of each RNA under partially denaturing conditions. It is likely that the presence of two genomes in one virion is advantageous for survival, providing an extra template that can be used when one RNA molecule is damaged and giving genetic variety to the progeny (11, 23). It has been suggested that the DLS in viral genomic RNA usually overlaps with a packaging signal (E/psi) (19). Therefore, it was difficult to assess whether viral RNA dimerization and packaging are independent events.

The partial RNA fragments of the 5′ region of a retrovirus genome transcribed and purified in vitro formed dimer molecules upon incubation in buffer without any proteins or cellular extract (19). Thus, the DLS has been inspected mainly by using in vitro transcription systems. In the case of human immunodeficiency virus type 1 (HIV-1), the 5′ untranslated region just downstream of the splicing signal was first reported to be a DLS, because in in vitro systems, the RNA fragments lacking this region have impaired ability to form a dimer (3, 31, 42). Recently, several groups reported another site within the 5′ untranslated region which was important for RNA dimerization in vitro. This site was located upstream of the 5′ splicing signal and named the dimer initiation site (DIS) (25, 35, 36, 41). The DIS consists of a stem-loop structure with a conserved palindromic sequence at the top of the loop. Two palindromic sites have been suggested to make a contact point, forming a kissing-loop complex to initiate dimer formation (25, 35, 36, 41).

Several studies of RNA dimerization in HIV-1 particles (in vivo) have shown different features of the dimer. The viral nucleocapsid protein (NC) or Gag precursor protein is suggested to alter the secondary structure of the RNA molecule and to stabilize RNA dimers, like molecular chaperons (13, 14, 16, 17). It has been reported that a mutation introduced around the DIS/DLS site did not affect dimer stability in vivo (6, 9, 39) and that a region far from the DIS/DLS affected dimer formation in the retrovirus genome (39, 43). Electron microscopic observation revealed that the HIV-1 RNA genome contains a central DLS and additional loop structures within each monomer subunit (22), suggesting that HIV-1 RNA contains more than one contact point. Thus, there are many discrepancies between the in vitro and in vivo data on HIV-1 RNA dimerization.

Previously, several mutants were generated with a duplicated 5′ region (1,000 bases) of viral genome containing the packaging signal-DLS region (E/DLS) at various ectopic positions of RNA, and their packaging abilities and dimer formation in the particles were examined (38). In the mutant virions, monomeric forms of virion RNA, which were totally absent

* Corresponding author. Mailing address: Department of Viral Infections, Research Institute for Microbial Diseases, Osaka University, 3-1 Yamadaoka, Suita City, Osaka 565-0871, Japan. Phone: 81-6-6879-8348. Fax: 81-6-6879-8347. E-mail: sakuragi@biken.osaka-u.ac.jp.

from the wild-type virions, were observed. This suggested that the 5′ region of the genome indeed plays an important role in RNA-RNA interaction during virion formation. In this study, we utilized this system to assess the exact location of the DIS/DLS of HIV-1. Portions of stem-loop U5/L or stem-loop 1 (SL1) were sequentially deleted, and the effects of these mutations on RNA dimerization and encapsidation efficiency were analyzed.

MATERIALS AND METHODS

Constructs. The replication-competent HIV-1 proviral clone pNL4-3 (1) and pMSMBA (32), a derivative of pNL4-3, were used as the progenitors for all the mutants described below. pNL4-3 was digested with *Nhe*I, treated with T4 DNA polymerase, and self-ligated with T4 DNA ligase to construct pNLNh. Therefore, pNLNh carries a 4-base insertion mutation within the *env* region, and Env protein expression is abrogated.

To construct pDDNBA, the plasmid pGEM-MM (38) was digested with *Bam*HI and *Acc*I and treated with T4 DNA polymerase, and an ~0.5-kbp fragment including the 5′ leader region of HIV-1 was isolated. This fragment was ligated into the T4 DNA polymerase-treated *Nhe*I site of pNL4-3 to construct pDDNBA. The fragment was in its original orientation.

To construct pdR/U5-BA, pdU5/L-BA, pdPBS-BA, and pdM-BA, the plasmids pdR/U5, pdU5/L, pdPBS, and pdM (34) were digested with *Not*I, treated with T4 DNA polymerase, and then digested with *Spe*I. Fragments of ~1.5 kbp, from the 5′ leader region to the *gag* region, were isolated from these plasmids and exchanged with the *Aat*II-*Sph*I fragment of pDDNBA to construct pdR/U5-BA, pdU5/L-BA, pdPBS-BA, and pdM-BA, respectively.

To construct pdLA1, a two-step PCR amplification was performed to introduce the mutation. The template for PCR was pNLdSpNc, which was generated by removing the *Spe*I-*Nco*I fragment of pNL4-3. The first pair of primers used was a sense primer, 432F (5′-GCAGCTGCTTTTTGCCTGTAC-3′), and an antisense primer, dLA1R (5′-GATTTTCCAACTGATCTGAGGGATCTCTA-3′), and the second pair was a sense primer, dLA1F (5′-TAGAGATCCCTCA GATCAGTTGGAAAATC-3′), and an antisense primer, 783R (5′-CCTTCTA GCCTCCGCTAGTC-3′). Two amplified fragments were isolated, mixed, and used for the second PCR with primers 432F and 783R to generate the mutated fragment. This fragment was digested with *Sac*I and *Bss*HII and inserted into the corresponding position in pNLdSpNc to construct pdLA1sub. The plasmid pdLA1sub was then digested with *Aat*II and *Sph*I, and an ~3.0-kb fragment was isolated and inserted into the corresponding position in pNLNh and pDDNBA to construct pdLA1 and pdLA1-BA, respectively.

The mutant constructs pdLA2 or pdLA2-BA, pdLA3 or pdLA3-BA, and pdLB3 or pdLB3-BA were constructed by the same method as pdLA1 or pdLA1-BA but using different primer pairs. For pdLA2, the first pair was a sense primer, 432F, and an antisense primer, dLA2R (5′-CTGCTAGAGATTTTCG GATCTCTAGTTACC-3′), and the second was a sense primer, dLA2F (5′-GG TAACTAGAGATCCGAAAATCTCTAGCAG-3′), and an antisense primer, 783R. For pdLA3, the first pair was a sense primer, 432F, and an antisense primer, dLA3R (5′-CGAGATCTCCTCTGGCACCAGAGTCACACAAC-3′), and the second was a sense primer, dLA3F (5′-GTTGTGTGACTCTGGTGCC AGAGGAGATCTCG-3′), and an antisense primer, 783R. For pdLB3, the first pair was a sense primer, 432F, and an antisense primer, dLB3R (5′-GGGATC TCTAGTTCGGGCACACAC-3′), and the second was a sense primer, dLB3F (5′-GTGTGTGCCCGAACTAGAGATCCC-3′), and an antisense primer, 783R.

To construct pdLB2 and pdLB2-BA, the plasmid pNLdSpNc was amplified with primers 432F and dLB2R (5′-GTGCGCGCTTCAGCAAGCCGAGTCCT GCGTCGCCAACACAACAGAC-3′), and the amplified fragment was digested with *Sac*I and *Bss*HII and exchanged with the corresponding fragment of pNLdSpNc to construct pdLB2sub. The plasmid pdLB2sub was digested with *Aat*II and *Sph*I, and the resultant 3.1-kb fragment was isolated and inserted into the corresponding position in pNLNh and pDDNBA to construct pdLB2 and pdLB2-BA, respectively. The mutant constructs pdLB4 and pdLB4-BA were constructed by the same method as pdLB2 and pdLB2-BA but using 432F and dLB4R (5′-GTGCGCGCTTCAGCAAGCCGAGTTTACTTTCGCTTTC-3′) as the primers.

The series of mutant constructs pdLC1, pdLC2, and pdLC3 and the series pdLC1-BA, pdLC2-BA, and pdLC3-BA were constructed similarly to pdLA1-BA or pdLA1-BA but with different primer pairs: dLC1F (5′-GGAGA TCTCTCTCGGCTTGCTG-3′) and dLC1R (5′-CAGCAAGCCGAGAGAGA TCTCC-3′), dLC2F (5′-GGAGATCTCTCAGGACTCGGCTTGCTG-3′) and dLC2R (5′-CAGCAAGCCGAGTCCTGAGAGATCTCC-3′), and dLC3F (5′-GGAGATCTCTCGACGCTCGGCTTGCTG-3′) and dLC3R (5′-CAGCAAG CCGAGCGTCGAGAGATCTCC-3′) were used for pdLC1 or pdLC1-BA, pdLC2 or pdLC2-BA, and pdLC3 or pdLC3-BA, respectively.

The construction of pS1, pBsS1, pBST2, and pBsT6 was described elsewhere (34, 39). These plasmids were digested with *Not*I, treated with the T4 DNA polymerase, and digested with *Spe*I. Fragments of ~1.5 kb, from the 5′ leader region to the *gag* region, were isolated and ligated with the *Aat*II-*Sph*I fragment of pDDNBA to construct pS1-BA, pBsS1-BA, pBsT2-BA, and pBsT6-BA.

To construct the mutant pdL1, a two-step PCR was performed using two pairs of primers. The first pair was 432F and dL1R (5′-CGCCCCTCGCCTCGCCG AGTCCTGC-3′), and the second pair was dL1F (5′-GCAGGACTCGGCGAG GCGAGGGGCG-3′) and 970R (5′-GTATTTGTCTACAGCCTTCTG-3′). The plasmid pNLdSpNc was used as a template for amplification with these pairs of primers, and two amplified fragments were isolated and mixed. The mixed fragments were then used as templates for the second step of PCR with the primers 432F and 970R, and the amplified fragment was digested with *Sac*I and *Acc*I. The resulting 0.47-kb fragment was isolated and inserted into the corresponding position of pNLdSpNc to construct pdL1sub. The plasmid pdL1sub was digested with *Aat*II and *Sph*I, and the fragment containing the mutation was inserted into the corresponding position in pNLNh and pDDNBA to construct pdL1 and pdL1-BA, respectively.

Three additional plasmids, pGEM634, pGEM634T2, and pGEM634T6, were constructed as templates for in vitro transcription. Each of the plasmids pNLdSpNc, pBsT2, and pBsT6 was used as a template for amplification with the primers PBS-F (5′-AGTGGCGCCCGAACAGGGAC-3′) and 1000R (5′-CTG TCTGAAGGGATGGTTG-3′). The amplified fragments were isolated and ligated with pGEM-Teasy vector (Promega) to construct pGEM634, pGEM634T2, and pGEM634T6, respectively.

Transfection. 293T cells (18) (~7×10^6) were seeded on dishes (diameter, 150 mm) on the day before transfection. Plasmid DNA (10 μg) was transfected into the cells using the calcium phosphate precipitation method (2). The day after transfection, the medium was replaced with fresh Dulbecco's modified Eagle's medium supplemented with 10% fetal calf serum.

Isolation of RNA from cytoplasm and virions. Forty-eight to 72 h after transfection, the medium and cytoplasmic RNA were collected concurrently as described elsewhere (32). Virions in the medium were collected by centrifugation (100,000 × *g*; 2 h), and the viral pellet was resuspended in TSE (10 mM Tris-HCl [pH 7.4], 100 mM NaCl, and 1 mM EDTA). The physical virus titer was determined using an enzyme-linked immunosorbent assay kit to quantitate CA-p24 (ZeptoMetrix, Inc.). To isolate RNA from particles, virions were disrupted by the addition of sodium dodecyl sulfate (SDS) to 1% and treated with proteinase K (300 μg/ml) at room temperature for 60 min, followed by Tris-EDTA-saturated phenol-chloroform extraction, chloroform extraction, and ethanol precipitation.

Northern blotting analysis. Pelleted RNA was resuspended in T buffer (10 mM Tris-HCl [pH 7.5], 1 mM EDTA, 1% SDS, 100 mM NaCl, and 10% formamide), and the thermostability of dimeric viral RNA was determined by incubating RNA aliquots for 10 min at the temperatures indicated in Fig. 2 (39). The proportions of the dimer and monomer were measured by electrophoresis at room temperature on a nondenaturing 0.75% native agarose gel in 0.5× Tris-borate-EDTA buffer (29). Field inversion gel electrophoresis was performed for better separation of large RNA molecules. The conditions for field inversion gel electrophoresis were as follows: forward, 5V/cm and 0.6s; reverse, 5V/cm and 0.1s. The agarose gel was then treated with 10% formaldehyde at 65°C before being washed with H_2O three times, and the RNA was blotted electrically onto a Hybond-N+ nylon membrane (Amersham Pharmacia Biotech UK, Ltd.).

RNA Northern hybridization analysis was performed as described previously (29). The plasmid T7pol (39) and T7 RNA polymerase (New England Biolabs) were used to synthesize the cRNA probe, which detects only unspliced viral RNAs, for Northern hybridization. Approximately 7×10^6 cpm of riboprobe per blot was used in the hybridization reaction. Hybridization was carried out in the presence of Rapid-Hyb buffer (Amersham Pharmacia). Membranes were washed extensively with 0.1× SSC (1× SSC is 150 mM NaCl and 15 mM sodium citrate [pH 7.0])– 0.1% SDS at 70°C. In experiments designed to assess the conversion of dimers to monomers, the relative amounts of both RNA species were quantitated with a BAS1000 imaging plate system and ImageGauge software (Fujifilm Co.).

RNase protection assay. The antisense probe (~10^8 cpm/mg) was synthesized by transcription of pGEM(600-1000) (33), pGEM634, pGEM634T2, and pGEM634T6 with T7 RNA polymerase (New England Biolabs) or by transcription of pT7HIV-1 410-910 (39) with SP6 RNA polymerase (Promega) following

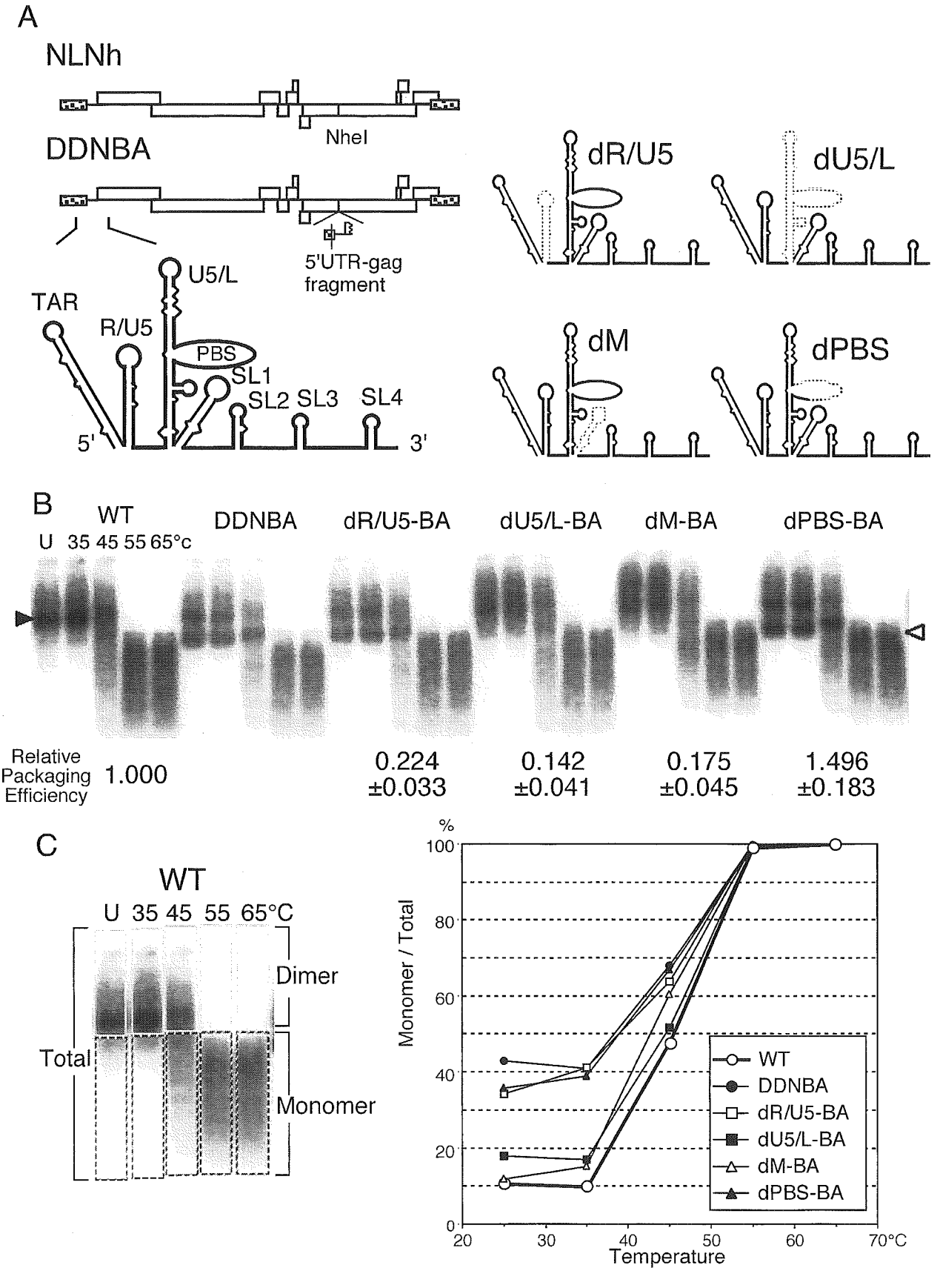
A
NLNh
NheI
DDNBA
5'UTR-gag
fragment
U5/L
TAR
R/U5
PBS
SL1
SL2 SL3
SL4
5'
3'
dR/U5
dU5/L
dM
dPBS
B
WT
U 35 45 55 65°c
DDNBA
dR/U5-BA
dU5/L-BA
dM-BA
dPBS-BA
Relative
Packaging
Efficiency
1.000
0.224
±0.033
0.142
±0.041
0.175
±0.045
1.496
±0.183
C
WT
U 35 45 55 65°C
Dimer
Total
Monomer
%
100
80
60
40
20
0
Monomer / Total
20
30
40
50
60
70°C
Temperature
WT
DDNBA
dR/U5-BA
dU5/L-BA
dM-BA
dPBS-BA

linearization with *Not*I [pGEM(600-1000)], *Spe*I (pGEM634, pGEM634T2, and pGEM634T6), or *Sal*I (pT7HIV-1 410-910) as described previously (30). To serve as size markers for denaturing polyacrylamide gels, *Hpa*II-digested fragments of pGEM3Zf (+) were ^{32}P end labeled (30). One-fifth of the virion-associated RNA or 10 μg of the cytoplasmic RNA preparation was mixed with 8 × 10^4 Cerenkov counts of ^{32}P-labeled antisense RNA and precipitated with ethanol. RNase protection assays were performed using an RPA III RNase protection assay kit (Ambion, Inc.). After electrophoresis in 5% polyacrylamide–8 M urea gels, the quantitation of various protected RNA species was achieved with the BAS1000 imaging plate system and ImageGauge software. The relative packaging efficiency was calculated by the following formula: relative packaging efficiency = (unspliced RNA of the mutant in virion/that in cytoplasm)/(unspliced RNA of the wild type in virion/that in cytoplasm).

The antisense probes from pGEM634, pGEM634T2, and pGEM634T6 were used to distinguish viral RNA of BsS1, BsT2, and BsT6, respectively, from that of the wild type. The probe from pT7HIV-1 410-910 was used to detect viral RNA of dR/U5 and dLB3. Other mutant RNAs were detected by the probe from pGEM(600-1000).

RESULTS

Contribution of 5′ stem-loops to RNA dimerization of HIV-1. In the 5′ untranslated region of HIV-1 RNA, the RNA is predicted to form seven stem-loop structures (TAR, R/U5, U5/L, SL1, SL2, SL3, and SL4) (7, 34). These stem-loops play important roles in viral genome packaging. On the other hand, it is still unclear whether these stem-loops are required for genome dimerization (6, 9, 39). We recently reported a series of HIV-1 mutant constructs containing an additional E/DLS region at the ectopic position (38). These mutant RNA molecules were packaged into virions as efficiently as the wild-type RNA. Nearly 40% of the mutant RNA molecules in virions, however, appeared to be monomeric, whereas the wild-type RNA molecules in virions were dimeric. We speculated that an additional E/DLS region at the ectopic position binds to the authentic E/DLS region on the same RNA molecules competitively, interfering with intermolecular dimer formation. If a mutation which abolishes RNA-RNA interaction is introduced in one of the E/DLS on this mutant, intramolecular interaction would also be abolished and monomeric RNA would not be observed in the virion. Even if such a mutation negatively affected packaging, the ectopic E/DLS would complement the packaging function. Thus, mutational analysis of this mutant could be used to precisely map the DIS/DLS on the HIV-1 RNA. In this study, we utilized this system to assess the precise location of the DIS/DLS of HIV-1.

We first constructed a plasmid called pDDNBA, a derivative of pDDN, for clearer identification of the DIS/DLS and easier manipulation of the mutant construction. The duplicated region of pDDNBA was 405 bases long, including all seven stem-loops at the 5′ end of the HIV-1 genome, whereas that of pDDN was >1,000 bases long, from the 5′ end to the middle of the *gag* gene. Polyadenylation signals and primer binding sites (PBS) in the ectopic fragment on pDDNBA were deleted to abolish undesired polyadenylation and ectopic initiation of reverse transcription. 293T cells were transfected with pDDNBA, and progeny virions were collected from the supernatant. The RNA encapsidation and dimerization abilities of the virions were compared with those of pDDN and the wild-type, pNLNh. The RNA-packaging efficiency of DDNBA was comparable to those of DDN and NLNh, and its RNA dimerization profile was indistinguishable from that of DDN. Therefore, the first 405 bases from the 5′ end of the HIV-1 RNA were sufficient to promote RNA-RNA interaction in virions (data not shown). Thus, we decided to use pDDNBA instead of pDDN as a progenitor of the mutants in the RNA dimerization assay. There were two E/DLS sites on the genome RNA of DDNBA, and we needed to decide which one would be mutated in this study. In a previous paper, it was speculated that the original E/DLS site on the mutant molecules worked more efficiently than the ectopic sites for the RNA-RNA interaction in the virion (37). In addition, we intended to observe the effect of the mutations on both dimerization and packaging efficiency. For packaging analysis, we have to use the mutants, which have only one E/DLS at the original position. Therefore, we decided to introduce mutations in the original E/DLS site of pDDNBA. For this purpose, we constructed the pDDNBA derivative plasmids pdR/U5-BA, pdU5/L-BA, pdM-BA, and pdPBS-BA, in which stem-loops R/U5, U5/L, and SL1 and the PBS, respectively, were deleted (Fig. 1A). Each mutant contained the deletion in the 5′ authentic E/DLS, whereas an additional E/DLS at the ectopic position was intact except for polyadenylation signals and the PBS, like pDDNBA. We compared the RNA dimerization profiles of these mutant virions to those of DDNBA and the wild type (Fig. 1B and C). The virion RNAs from dPBS-BA and dR/U5-BA formed monomeric RNA at low temperature, similar to that of DDNBA. This result indicated that the PBS and stem-loop R/U5 do not help to promote RNA-RNA interaction in virions, and we concluded that these regions were not included in the DIS/DLS at all. On the other hand, the RNAs produced by dU5/L-BA and dM-BA contained very little monomer, similar to that of the wild type. This result indicated that the U5/L and SL1 stem-loop regions are important for the formation of dimeric RNA in virions.

FIG. 1. Impact of a stem-loop deletion of the 5′ region of HIV-1 RNA on genome dimerization. (A) Diagram of the prototype plasmids NLNh and DDNBA and the 5′ regions of the stem-loop deletion mutants. The dotted lines represent deleted areas of RNA. (B) Representative ImageGauge image of RNA detected by Northern blotting. Aliquots of RNA extracted from virions were resuspended in T buffer, incubated for 10 min in parallel reactions at various temperatures, and then analyzed on a native agarose gel. The positions of dimeric and monomeric viral RNAs are indicated by a solid and open arrowhead, respectively. The various temperatures at which aliquots were incubated are indicated for the wild-type (WT) lane. Three or more independent experiments gave similar results. The relative packaging efficiency of each mutant is shown below its blot. The packaging efficiencies were calculated from the results for the mutants, which do not contain a second copy of E/DLS. The relative encapsidation efficiencies were calculated as the ratio of the amount of mutant genomic RNA to that of the wild type (pNLNh) in the virions, with normalization to the cytoplasmic levels of the two RNAs. The results represent means ± standard errors from at least three independent experiments. (C) Thermal-dissociation kinetics of dimeric viral RNAs shown in panel B. A schematic figure for dimer/monomer calculation is shown on the left. Each lane of the blot was separated into two parts, dimer or larger and monomer or smaller molecules. The relative amounts of monomeric and total RNAs in each lane were quantitated with ImageGauge, and the percentage of the total represented by monomeric RNA was calculated for each RNA sample. Lanes U, unheated samples.